Ann. Naturhist. Mus. Wien, Serie A	121	291–326	Wien, 15 Jan. 2019

Neotectonics and paragenesis – a case study from the Jedovnice Creek cave system in the Moravian Karst, Czech Republic

Vojtech A. Gregor[1], Jiří Havlík[2] & David Mikeš[3]

(with 30 figures and 2 tables)

Manuscript submitted on May 16th, 2018,
the revised manuscript on August 20th, 2018.

Abstract

The main passage of the Jedovnice Creek cave system in the Moravian Karst contains a number of atypical sections with a low, generally horizontal and flat ceiling. Usually leveled across dipping strata, these sections are limited to tectonically sunken blocks that are bounded by faults. These faults bear signatures of neotectonic, more specifically Pleistocene reactivation. Both the sinking and the sections are post-genetic with respect to the main passage. Within the sunken blocks, the ceiling of the main passage (or parts of it) was brought down into contact with the water body (water stream) and thus, exposed to the effects of paragenesis (also called antigravitational erosion (in this study more properly corrosion)). The original shape and features, namely positive relief, were removed – the ceiling was flattened. The present, superimposed morphology includes small solutional and erosional forms, typically inverse ceiling pots and scallops.

Keywords: neotectonics, speleogenesis, antigravitational corrosion, paragenesis, Moravian Karst.

Zusammenfassung

Die Hauptteile des Jedovnice-Fluss-Höhlensystems im Mährischen Karst enthalten eine Reihe von atypischen Abschnitten mit einer niedrigen, im Wesentlichen horizontalen und flachen Decke. Diese sind in der Regel auf eintauchende Schichten verteilt und beschränken sich auf tektonisch abgesunkene Blöcke, die an Störungen gebunden sind. Diese weisen Kennzeichen einer neotektonischen, pleistozänen Reaktivierung auf. Sowohl das Absinken als auch die Abschnitte selbst sind in Bezug auf die Hauptgänge der Höhle post-genetisch. Innerhalb der abgesunkenen Blöcke wurde die Decke der Höhlengänge (oder Teile davon) in Kontakt mit dem Wasser gebracht und

[1] VAG Geoscience Specialists, P.O. Box 192A, Prince George, BC V2L 4S1, Canada; e-mail: vageosciences@gmail.com

[2] ProfiGas, s.r.o., P.O. Box 19, Slavkov u Brna, 68401 Czech Republic; e-mail: jiri.havlik@profigas.sk

[3] Masaryk University, Faculty of Natural Sciences, Department of Geology, Brno, Czech Republic; e-mail: dmikes@mail.muni.cz

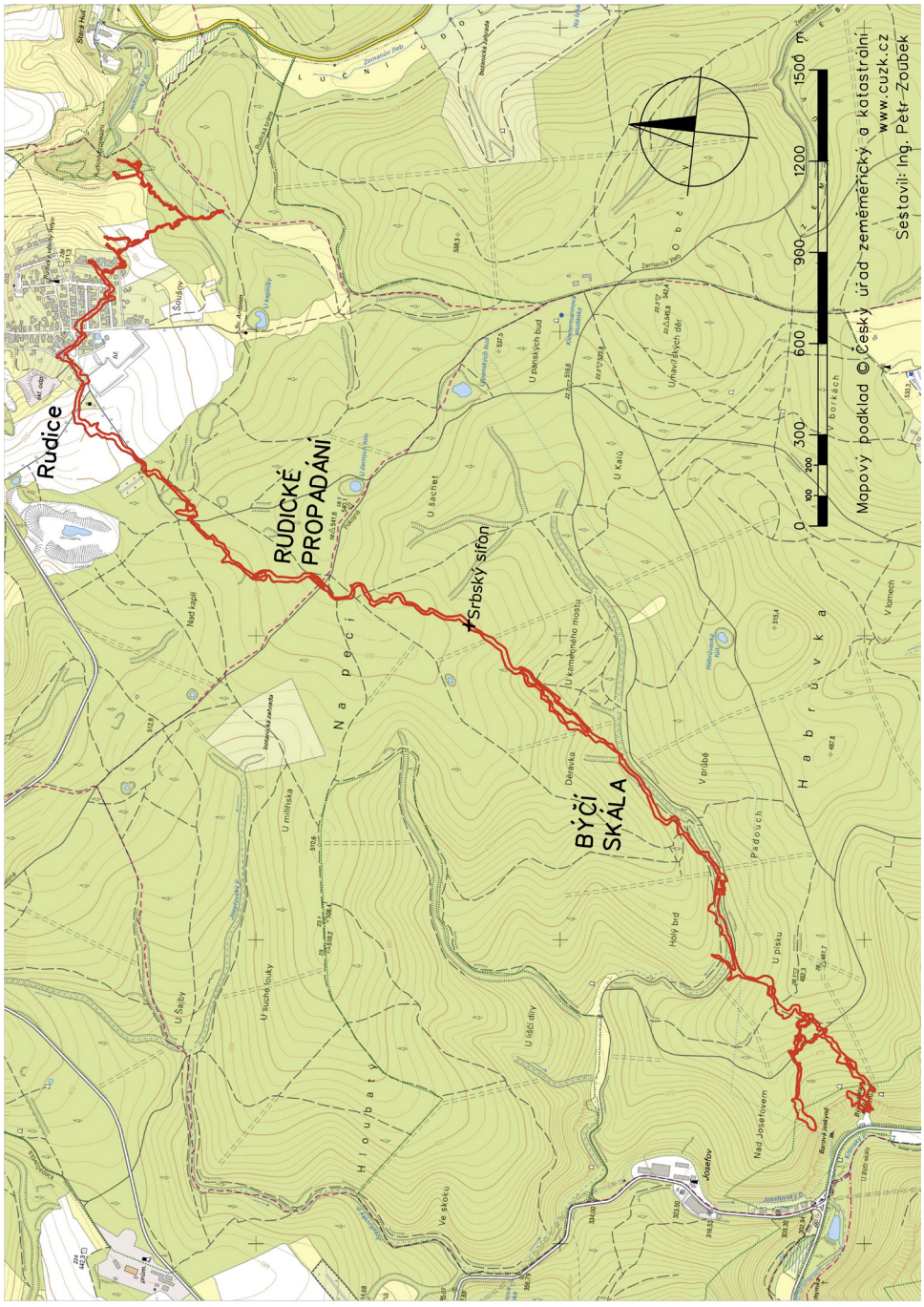


Fig. 1. Rudice Plateau and its cave system. The Serbian Siphon is the conventional dividing point between the Rudice Swallow Hole Cave (jeskyně Rudické propadání) and the Bull Rock Cave (jeskyně Býčí skála). Mapový podklad © Český úřad zeměměřický a katastrální, www.cuzk.cz (used with permission).

somit den Auswirkungen der „Paragenese“ ausgesetzt. Die ursprüngliche Form und Merkmale, nämlich positive Strukturen, wurden entfernt – die Decke wurde abgeflacht. Die vorliegende überlagerte Morphologie umfasst kleine Lösungs- und Erosionsformen, typischerweise inverse Deckenstrukturen und Fließfacetten. [Translated by Dr. Johannes MATTES, Secretary General of the Austrian Speleological Association, Fellow of the Austrian Academy of Sciences]

Schlüsselwörter: Neotektonik, Speleogenese, Antigravitationskorrosion, Paragenese, Mährischer Karst.

Introduction

Geological mapping of the Jedovnice Creek cave system (BURKHARDT 1973; BURKHARDT *et al*. 1975, 1977) revealed that the system (Fig. 1), especially the main passage of the Rudice Swallow Hole Cave and the Bull Rock Cave, contains a number of atypical sections with a low, generally horizontal and flat ceiling. Such sections are bounded by faults that intersect the passage. These faults contain brecciated fills that consist of primary calcite, varicolored clays and locally also of secondary calcite – both a result and evidence of repeated tectonic movements.

In the years 2013–2015, the present authors concentrated on a detailed study of the flat-roofed sections. The study focused on the flattening (leveling) mechanism and the possible role of fault tectonics (movement along pre-existing faults that occurred during or after the formation of the main passage) in the origin of these sections. This paper presents the results of this study. It also adds a new dimension to the conventional concept of paragenesis.

Abbreviations

The following is an alphabetical list of abbreviations of geographical toponyms and other terms that are used throughout this paper – in the text, figures and figure captions. Since this is an English language paper, the abbreviations are in English; the proper names are given first in English, then in Czech:

AVD – apparent vertical displacement (along faults)

BEL – Black Loams semi-siphon – Easter Cave – Library section

BIR – Broken-in Rock Cave, Prolomená skála

BL – Black Loams semi-siphon, polosifon U Černých hlín

BRC – Bull Rock Cave, jeskyně Býčí skála

DC – Dome with Chimneys, Dóm s Komíny

EC – Easter Cave, Velikonoční jeskyně

GnD – Giant Dome, Obří dóm

GnS – Giant Dome semi-siphon, polosifon z Obřího dómu

GtD – Gothic Dome, Gotický dóm

LB – Library w/entrance semi-siphon, the Peek; Knihovna se vstupním polosifonem Jukadlo

NBR – New Bull Rock Cave, jeskyně Nová Býčí skála

OBR – Old Bull Rock Cave, jeskyně Stará Býčí skála

PSbS – proper Serbian Siphon, vlastní Srbský sifon

RSH – Rudice Swallow Hole Cave, jeskyně Rudické propadání

SA – Saxon (Saxon-Alpine)

SbS – Serbian Siphon incl. Library, Srbský sifon s Knihovnou

SPE – Stretch of Preliminary End, Úsek předběžného konce

ss – semi-siphon

SS1 to SS3 – semi-siphons 1 to 3 in EC, polosifony 1 až 3 ve Velikonoční jeskyni

STR – Swum-through Rock Cave, Proplavaná skála

TB – Tablets and Beaches, Tabulky a Pláže

VA – Variscan

Note: the strike of planar geologic features is given in the eastern compass semicircle, 0º to 180º. For example, the symbol 160/80 SW or 160º/80º SW means a feature striking 160º (*i. e.*, 160–250º and dipping 80º to the south-west).

Survey methods

Unfolded longitudinal cross-sections (LXS) of the flat-roofed parts of the main passage are the backbone of this study. Four such LXS are presented, namely those of the Giant Dome semi-siphon (GnS), a section between the Gothic Dome and the Tablets (GtD-TB, including the BL, EC and LB), the Strech of the Preliminary End (SPE) and the BIR semi-siphon (see Fig. 2). Of these, the GtD-TB section is the longest, measuring *ca*. 550 m. Some 1800 measurements were taken in the survey and used in the construction of the LXS.

Supplementary measurement points were added to the main polygon trace; the distance between these points ranged from 2 m to 0.5 m, depending on the ceiling height and relief. Laser distance meter Leica Disto™ X310 with an accuracy of ± 1 mm was used in most measurements. In cases where the situation did not allow for the use of this instrument, particularly water depth measurements and the survey of the Serbian Siphon, calibrated steel rods and rulers were employed.

Software program Maple™15 was used to process the survey data and construct the LXSs. In these, the black line represents the cave ceiling, the blue line the reference plane (normal water level), and the red line the cave floor (top of sedimentary fill).

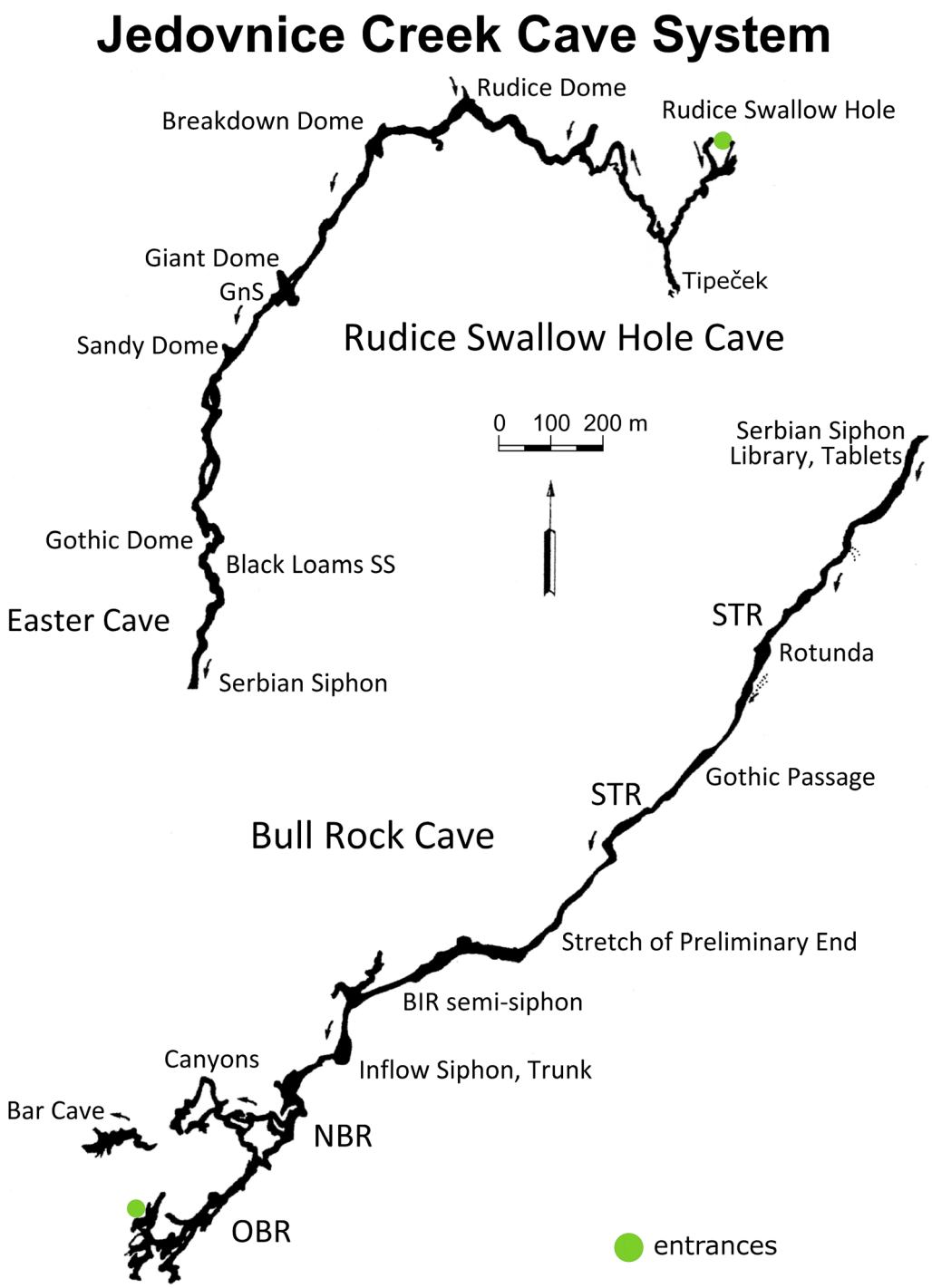


Fig. 2. Schematic map of the Jedovnice Creek cave systém – from MUSIL (1993), used with permission.



Fig. 3. Tunnel section of the main passage in the Bull Rock Cave (STR), upstream view. Photo by Philippe Crochet and Annie Guiraud, 2013 (used with permission).

The Jedovnice Creek cave system

The Jedovnice Creek cave system is situated in the central part of the Moravian Karst, 70–220 m beneath the surface of the Rudice Plateau (Gregor 2015). At a total length of some 13 km, the system is the second longest in the Czech Republic. It consists of four principal cave units (Figs 1 and 2), namely the Rudice Swallow Hole Cave (RSH), the Bull Rock Cave (BRC), the Bar Cave, and the karst conduits of the Josefov springs. The RSH formally consists of the geologically younger canyon part and the geologically older tunnel part (including the Easter Cave – EC). The BRC is comprised of the Old Bull Rock Cave (OBR), New Bull Rock Cave (NBR), Broken-in Rock Cave (BIR), and the Swum-through Rock Cave (STR).

The main passage of the system – originally a epiphreatic, tunnel-shaped channel that was later remodeled by gravitational erosion as well as corrosion from waters of the zone of vertical descendent circulation (meteoric waters descending from the surface of the karst plateau) – is 5.75 km long. The passage forms the greater part of the Rudice Swallow Hole and the Bull Rock Cave (Fig. 2). The present topography includes sections of the original tunnel passage (Figs 3 and 4), sections strongly remodeled by vertical corrosion (Fig. 5) and locally also by breakdown (Fig. 6), sections that follow prominent

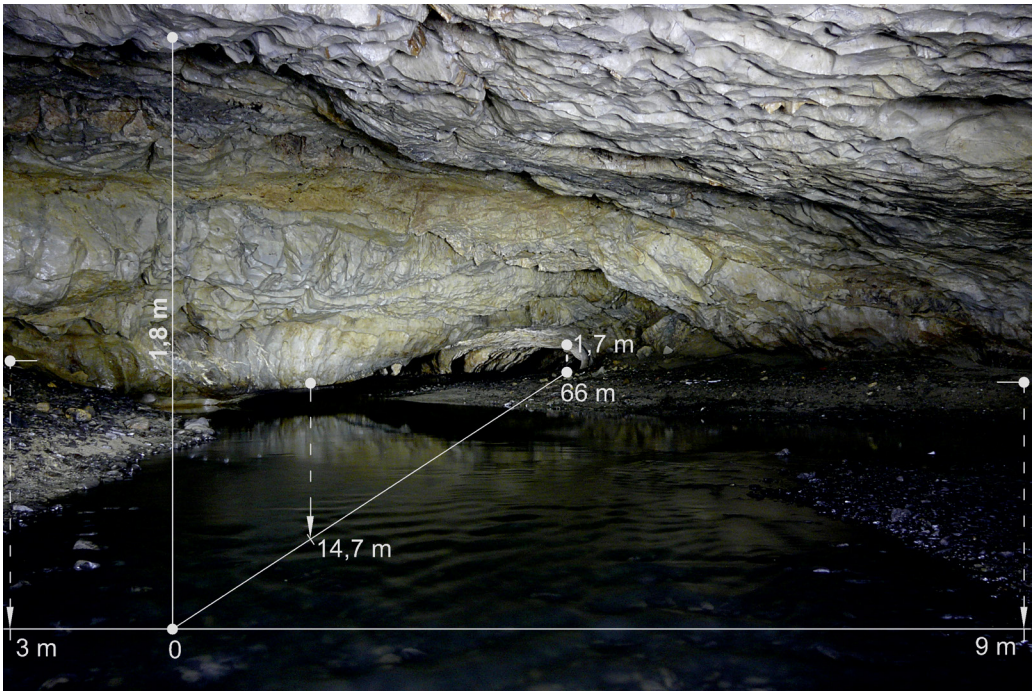


Fig. 4. Low profile, tectonically sunken and sediment-filled tunnel section of the main passage (in the background) in the Easter Cave (RSH), upstream view.



Fig. 5. Tunnel passage (a relict on the right) invaded and modified by vertical corrosion (STR), upstream view. Photo by Philippe CROCHET and Annie GUIRAUD, 2013 (used with permission).



Fig. 6. Tunnel passage modified by breakdown (BIR), downstream view. Photo by Philippe Crochet and Annie Guiraud, 2013 (used with permission).

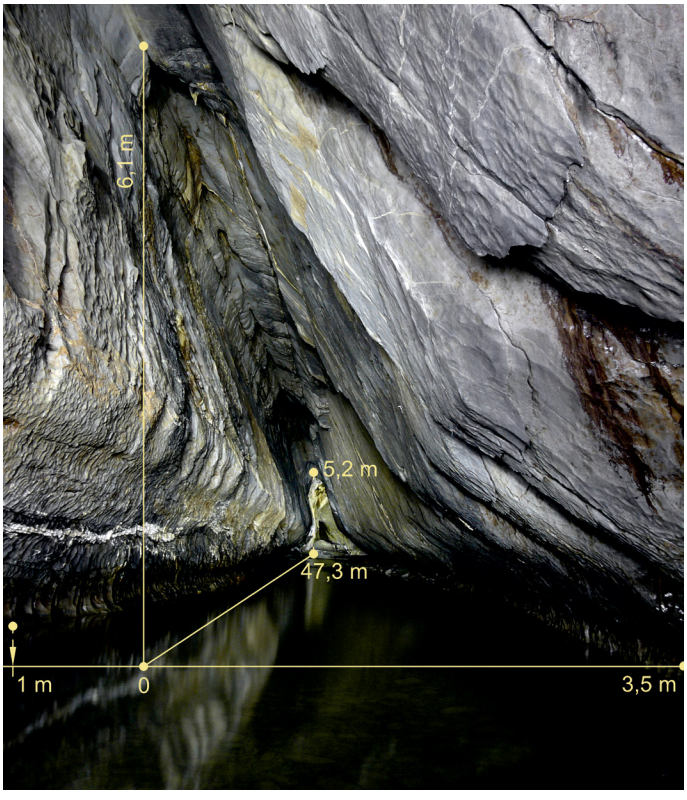


Fig. 7. Tectonically controlled section of the main passage: the Gothic Passage (STR), upstream view.

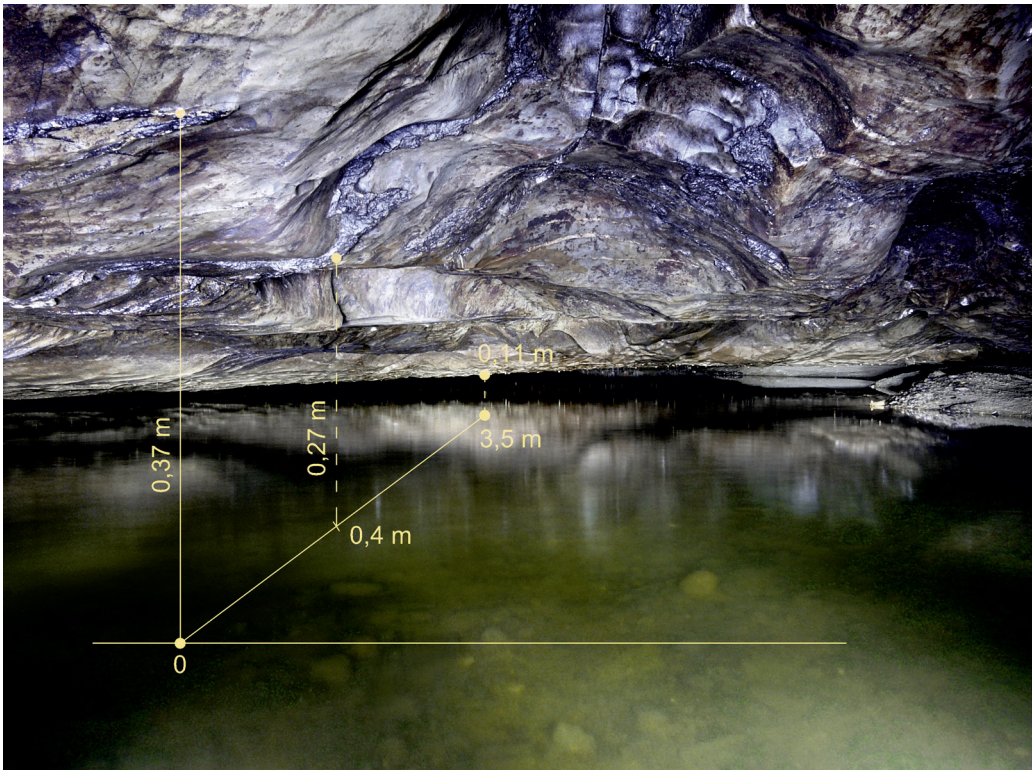


Fig. 8. Section with a low, flat ceiling: central part of the Black Loam semi-siphons (EC), upstream view.

structural elements (Fig. 7) and, finally, atypical sections with a low, flat ceiling (Fig. 8). The last mentioned type is commonly associated with semi-siphons (parts with a low convacuation space, usually several centimeters to a few decimeters in height; also termed half-siphons) that at increased water levels become siphons.

Geologic setting of the Rudice Plateau and the Jedovnice Creek caves

The limestone massif of the Rudice Plateau (Rudická plošina) is built by Devonian, Givetian to Frasnian limestones of the Macocha Formation (ZUKALOVÁ & CHLUPÁČ 1982), namely, from the base up, the Josefov Lm., the Lažánky Lm. (the Habrůvka cycle), and the Vilémovice Lm. (HLADIL 1983, 1986). The package includes so-called transitional strata between the Vilémovice and Lažánky limestones. This unit consists of alternating, centimeters to meters thick light-gray and dark-gray limestone layers and exceeds 100 m in total thickness (BURKHARDT *et al*. 1975). The dark-grey Lažánky Lm. contains 51 % CaO and 4.2 % MgO, and the light-grey Vilémovice Lm. 55 % CaO and 0.33 % MgO (average values). The complete stratigraphy and chemical composition of the Macocha Formation are presented in GREGOR (2015).

The massif is folded and fractured. The main deformation took place during the uppermost Viséan (Sudetian) phase of the Variscan (Hercynian) orogeny. The fractures – namely faults and with them associated master joints and joint zones – belong to two systems: the older Variscan system (primaries striking ESE-WNW, 120–140°, and orthogonals NE-SW, 30–50°), and the younger Saxon-Alpine system (Tab. 1, symbols VA and SA, respectively). Saxon-Alpine primaries (NNW-SSE, 160° ± 10°) are the most

Tab. 1. Main tectonic events and fracture systems in the Moravian Karst. Notes: Fracture strike directions, *e. g.*, **120–132°**/35–42° – primaries (bold print) and orthogonals (conjugate features). Orogeny: E: early, M: middle, L: late. PC: primary calcite, SC: secondary calcite. G–I: stagmalite generation I (see Tab. 2). V1, V2, A1, A2, B1, B2: vein and fracture calcite types. For full version of the table and description of calcite fills see Gregor (2015).

Tectogenesis		Moravian Karst – main events	Tectonic fractures			Principal fracture mineral fills
			Established (new)	Reactivated (older)	Apparent (cumulative)	
Neotectonics NT	Post-Upper Miocene to Recent	Reactivation of older fractures	–	160–170° 120–132° 10–23°	–	G-I (SC) A11 (PC)
Alpine (Alp-Carpathian) AL	Paleocene to Upper Miocene	SA-AL tectogenesis; Rudice sunken block, Blansko Graben Valchov Graben	**160–170°**/70–80°	**136–145°**/44–56° 100–112°/**10–23°** (reversal of primaries) 120–132°/30–42°	**150–170°**/60–80° (Saxon-Alpine system)	A1, A2, B1 (hydrothermal fracture calcites); limonite, hematite, goethite, pyrite
Saxon SA	L-Lower to Upper Cretaceous E-Upper Jurassic		**150–160°**/60–65°			
Variscan (Hercynian) VA	L-Permian M-Upper Carboniferous (Krusne Mountains and Asturian phases)	VA fracture tectogenesis (post-orogenic adjustments); Boskovice Furrow, Macocha main faul	**120–132°**/30–42° (Late Variscan system) calcite veins (bulk)	136–145°/**46–54°** **356–6°**/85–96° (reversal of primaries)	100–145°/10–46° (Variscan systems, primaries undistinguished)	A2, B1, B2, V2 (hydrothermal calcites); some Fe-mineralization; Cu-ore in basal clasts
(BM: Early Variscan metallogenetic epoch)	E-Lower Carboniferous (Sudetian phase, Uppermost Visean)	Main deformation of the limestone complex (compression and folding)	Calcite veinlets (late stage of the main deformation); fold joints *ac*, *bc*, {*h*0*l*}	–	–	V1 (hydrothermal veinlet calc); in BM Cu-ore w/ SiO_2, $CaCO_3$ and barytes

prominent tectonic lines. They form the fracture zone of the Blansko Graben and dominate the Rudice sunken block (Fig. 9, insert B; Fig. 10). The block is noted for well-preserved fossil tropic karst (paleokarst) of the Lower Cretaceous age, with depressions up to 140 m deep (BURKHARDT 1974; BOSÁK 1980).

Fractures, both faults and joints (the latter including bedding and fold joints, particularly fold axial cleavage joints *bc* and to them perpendicular extension joints *ac*), have exercised strong control over the origin and development of the cave system. Figure 9 portrays major structural features of the Rudice Swallow Hole Cave.

Tab. 2. Calcite speleothem chronology. Notes: I (the oldest) to VI (the youngest) – generations of calcite speleothems in the Moravian Karst caves (from GREGOR, unpublished manuscript).

Chronology			**Generations**						**Comments**
Geological		Absolute (ka)	VI	V	IV	III	II	I	
Holocene	Recent	2.0	I	↑	↑	↑			VI: 1890–1989
	Subrecent		I	I	I	I			average growth
	Subatlantic		I	I	I	I			rate 0.69 mm/a.
	Subboreal	0.7		I	I	I			
	Epiatlantic	1.2		I	I	I			IV and V: average
	Atlantic	4.0		I	I	I			growth rate for
	Boreal	6.0		I	I	I			stalagmites
Pleistocene	Late Würm			I	I	I			0.15 mm/a.
	(Alleröd	11		I	I	I			
	Interstadial to			I	I	I			III: average growth
	Bölling Inter-	13			I	I			rate for stalagmites
	stadial, W2/W3)				I	I			0.1 mm/a.
	Early Würm	50				I			
	(Pleniglacial:						I		II: consists of two
	Brörup Inter-						I		discernible sub-
	stadial, W1/W2						I		generations,
	to Riss/Würm	80					I		IIa and IIb (older).
	Interglacial-Eem)						I		
	Riss complex	130						I	
	Mindel/Riss Inter-	320						I	I: consists of three
	glacial							I	discernible sub-
	Mindel complex	420						I	generations, Ia, Ib
	Mindel/Günz	500						I	and Ic (the oldest).
	Interglacial							I	
	Günz-Danub	600						I	
	complex							I	

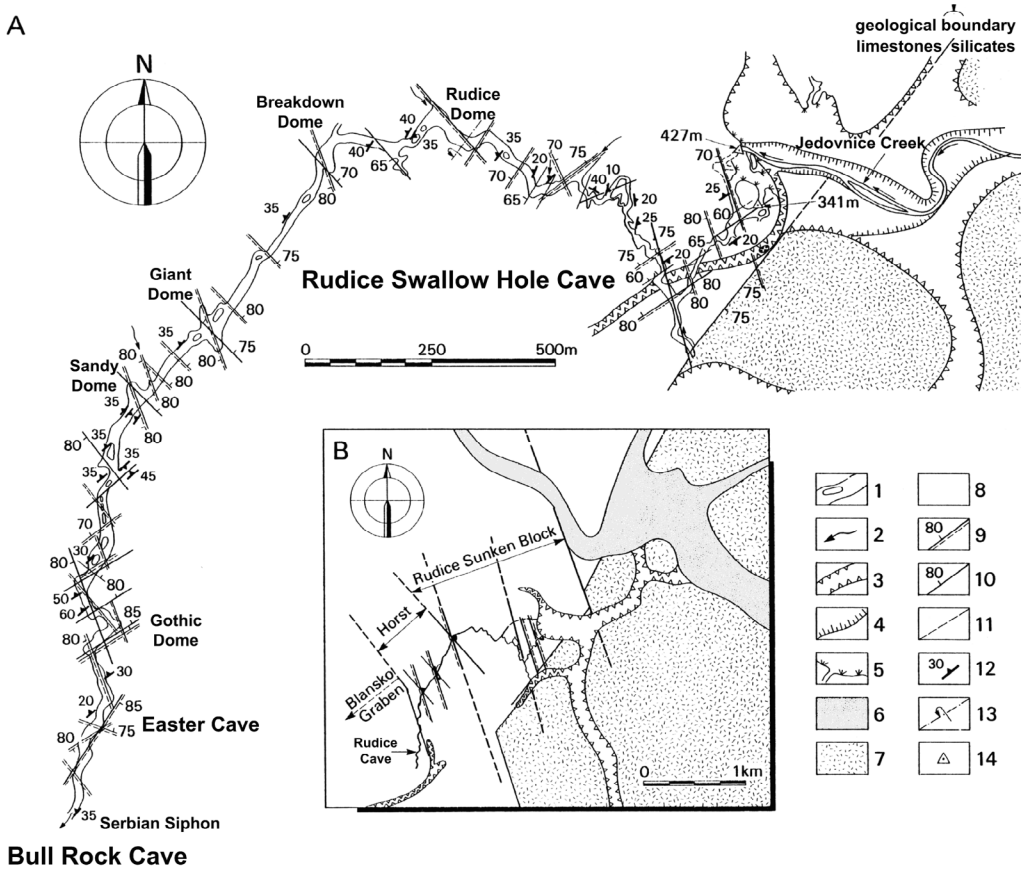


Fig. 9. Major structural features of the Rudice Swallow Hole Cave (A) and the Rudice Plateau (B). Explanatory notes: 1: cave passages, 2: surface and underground water stream courses, 3: surface erosional cuts w/Quaternary sediments, 4: Quaternary gravel terraces and alluvia, 5: outcrops of Devonian limestone, 6: Neogene sediments (valley fill), 7: Lower Carboniferous silicates (Culm), 8: Devonian limestone, 9: faults and associated joint zones, strike and dip, 10: faults, strike and dip, 11: inferred tectonic lines, 12: limestone beds, strike and dip, 13: overturned recumbent fold, 14: leveling points, altitude above sea level in meters. Authors: R. BURKHARDT and V. A. GREGOR (BURKHARDT *et al*. 1975, 1977).

The limestone surface of the plateau is covered with thick Mesozoic, Tertiary and Quaternary deposits. These deposits, namely sands, silts and clays of the Lower Cretaceous Rudice Formation (also called "Rudice beds"), chert detritus and loess loam, sink and/or are washed down into the cave system by means of vertical conduits, mostly cave chimneys (GREGOR 2013, 2014a, 2014b). Tens of meters thick Rudice beds have been locally mined for use in the foundry and ceramics industries.

The cave sedimentary fill is represented largely by allochthonous Quaternary fluvial sediments – gravel, sandy gravel, sand, silt and clay of the Culm provenience (siliceous

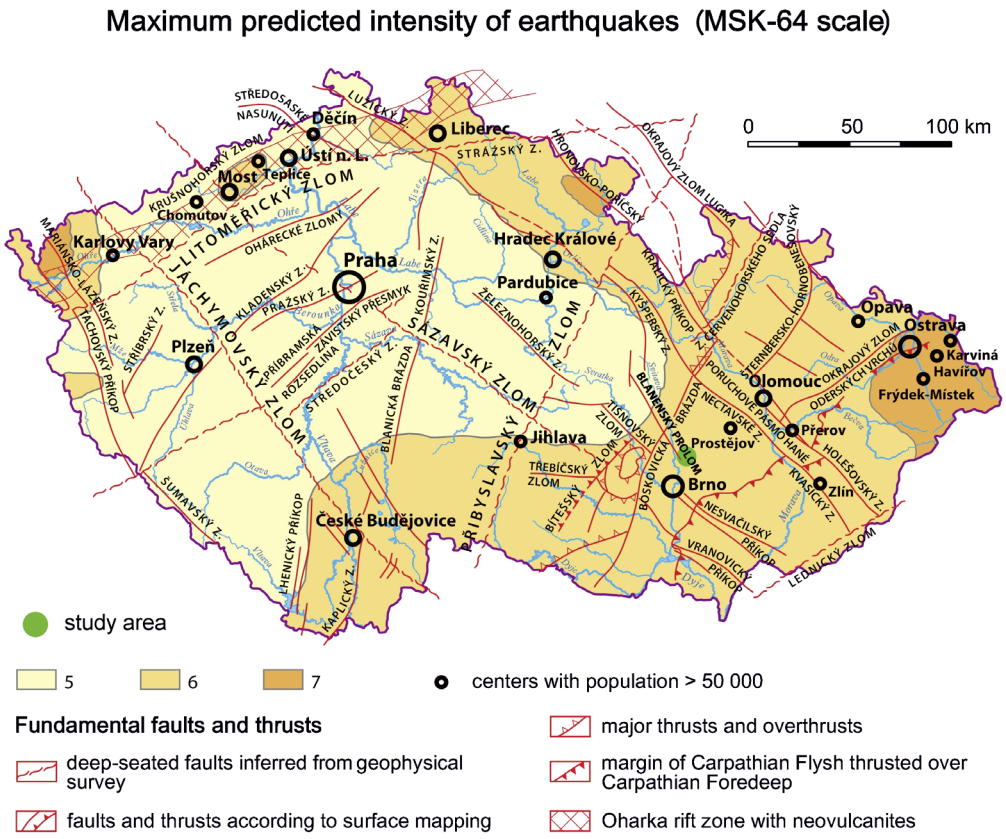


Fig. 10. Fundamental fault and thrust network of the Czech Republic and maximum predicted intensity of tectonic earthquakes. Blanenský prolom = Blansko Graben. The SE part of the graben extends into the study area – the central part of the Moravian Karst, the Rudice Plateau (courtesy of the Czech Academy of Sciences, Institute of Geophysics, 2012).

shale and graywacke of the Drahany Upland; MUSIL 2009). The gravel fraction contains a substantial amount of slag. This slag comes from a large deposit in the blind Rudice-Jedovnice Valley – a reminder of iron works that operated there from 1746 to 1890. The slag causes corrasion (abrasion) of speleothems within the water reach (the hydrodynamic zone of horizontal circulation and that of seasonal and flood/storm fluctuation according to the classification of hydrodynamic zones in carbonate rocks by GREGOR 1986) and contributes to sediment accumulation in, and plugging of, low profile passages. The two-way traverse of the main passage of the Bull Rock Cave – Rudice Swallow Hole complex by J. HAVLÍK and D. MIKEŠ on the 4th of July, 2015 (MIKEŠ *et al.* 2015) was probably the last one – that is, if the present high rate of sedimentation continues. The Easter Cave with the Serbian Siphon – a *ca*. 450 m long section of the main passage (Fig. 2) – is presently impassable.

Neotectonics and the age of the Moravian Karst caves

The term "neotectonics" refers to the youngest period of tectonic evolution that extends up to the present (Vita-Finzi 1986). The beginning of neotectonic activity during the Cenozoic may be regarded as having commenced when characteristic changes in the tectonic evolution of a region have occurred for the last time (Becker 1993) or, in other words, after its last orogeny or significant tectonic setup (Pavlides 1989).

In the Bohemian Massif, the Variscan orogeny was the last orogenic event and the Saxon (Saxon-Alpine) tectogenesis the last major tectonic event. Saxon movements commenced in the Lower Cretaceous and faded out during the Middle Miocene. Consequently, all post-Lower Badenian (certainly post-Middle Miocene) tectonic movements and deformations are considered neotectonic; they result from continuing Alpine (Alpine-Carpathian) tectonic activity. According to Hrádek & Ivan (1974), Pliocene and Pleistocene movements played an important role in the present-day geomorphology of the Bohemian Massif; these authors presented a map of neotectonic fold-fault morphostructures in the wider surroundings of the city of Brno (see also Ivan 1996). Kettner (1960) suggested that the youngest tectonic movements took place between the Pliocene and Pleistocene epochs, and between the Early and Late Pleistocene; they occurred along reactivated older tectonic lines. Panoš (1961) alleges that minor movements occurred still during the Late Pleistocene and Holocene, connoting that they extend into the present.

The Moravian Karst is situated at the seismically active southeastern margin of the Bohemian Massif, in the foreland of the Western Carpathians. The sedimentary rocks of the Moravian Karst overlie the crystalline rocks (mostly granitoids) of the Young Cadomian igneous Brno Massif – a unit of the Bohemian Massif (Dudek 1980; Hanžl & Melichar 1997). Neotectonic stress fields in the Bohemian Massif (including the Brno Massif) have reactivated older faults, mainly those striking NW-SE and NNW-SSE (Fig. 10; Skácelová & Havíř 1998; Špaček *et al*. 2006; also Musil 1997). Recently, they are revealed by fault earthquakes up to 4.5 in magnitude on the Richter scale (Květ 1974) and 7 on the MSK-64 scale (Fig. 10). Neotectonic stresses reactivated also VA and SA orthogonals, especially fractures striking NNE-SSW to ENE-WSW (Tab. 1). Špaček *et al*. (2017) describe Pleistocene deformations, including speleothem fracturing in caves of the North Moravian Karst (Bábek *et al*. 2015), along reactivated Variscan orthogonals.

The age of the valley and cave network of the Moravian Karst is subject to ongoing discussion (Gregor 1981, 2015; Dvořák *et al*. 1993; Dvořák 1994). As far as the age of the main cave levels is concerned, two basic hypothesis have been formed:

- pre-Lower Badenian (Paleogene to Middle Miocene),
- post-Lower Badenian (Pliocene to Holocene).

Concerning the main passage of the Jedovnice Creek cave system, the primary tunnel form is post-Lower Badenian, most probably Pleistocene in age (Burkhardt 1973, 1974; Burkhardt *et al.* 1975; Gregor 1981, 2015). On the basis of a comparative study

of sedimentary fills of the Bull Rock and Bar caves as well as those of the Křtiny Valley in the resurgence area of the Jedovnice Creek (Fig. 1), Hypr (1977) places the age of the passage to the Mindel-Riss interglacial or, alternatively, the Riss glacial period (personal comm., 2012).

Neotectonics of the Rudice Plateau and the Jedovnice Creek cave system

In the Rudice Plateau area, neotectonic stress fields reactivated Variscan and, predominantly, Saxon primaries (120–140° and 150–160°, respectively: Tab. 1). The last-mentioned fractures are associated with the Blansko Graben (Fig. 10) – a trench-like structural low that contains tectonically sunken deposits of Late Cretaceous (Cenomanian and Turonian) age. The graben's western marginal fault (Fig. 9, insert B) displays an apparent vertical displacement (AVD) of *ca*. 100 m. To the east, this amplitude is counterbalanced by five faults, each with 15–20 m AVD (Burkhardt 1974; Bosák 1980).

Neotectonic movements along the primary fractures of the Blansko Graben – Rudice Plateau area were mostly normal in nature. Boreholes in the Quaternary fluvial sediments in the south-central part of the graben indicate Pleistocene (probably Middle Pleistocene) fault movements with an AVD as high as 12 m (Dvořák *et al*. 1993). In the cave system of the Jedovnice Creek, the amplitude of the AVD, as inferred from the morphology of the main passage, is estimated at some < 2 m to 4 m. The surface projection of some faults detected in the underground was traced using geophysical electromagnetic methods (Gregor & Princ 1975a, 1976).

Faults in the limestone strata of the Rudice Plateau (Moravian Karst generally) are usually filled with, in a descending order of occurrence, primary calcite, gouge, and mylonite. The term "primary calcite" has been applied by Gregor (1975), Gregor & Princ (1975b, 1977), Lysenko & Slačík (1975) and Slačík (1975, 1982) to both granular and crystalline calcite that occurs in the limestone mass in the form of veinlets, veins and fracture fills. Typical fault fills contain hydrothermal calcite of the A1, A2, B1 and/or B2 type (Tab. 1) with characteristic physical and chemical properties (Gregor 2015: tabs 4 to 6 ibid.).

Repeated movements along the faults resulted in, and are indicated by, brecciation of the original primary calcite fills, deformation of calcite crystals and grains (locally with tectonic striation) and recrystallization. Calcite breccias typically contain multiple generations of calcite cement. The youngest generation is undeformed, usually light-honey colored and, according to Gregor (1976), of neotectonic or rather post-neotectonic origin. Calcite fills, both intact and brecciated, can exceed 10 m in thickness.

Calcite fracture fills commonly contain iron oxides (hematite), hydrous oxides (limonite and goethite), and sulfides – mostly pyrite, less chalcopyrite, and rarely galenite and Cu-sulfides (Gregor 1976; Slobodník 2000). This mineralization can be macroscopic or microscopic, disseminated or zonal.

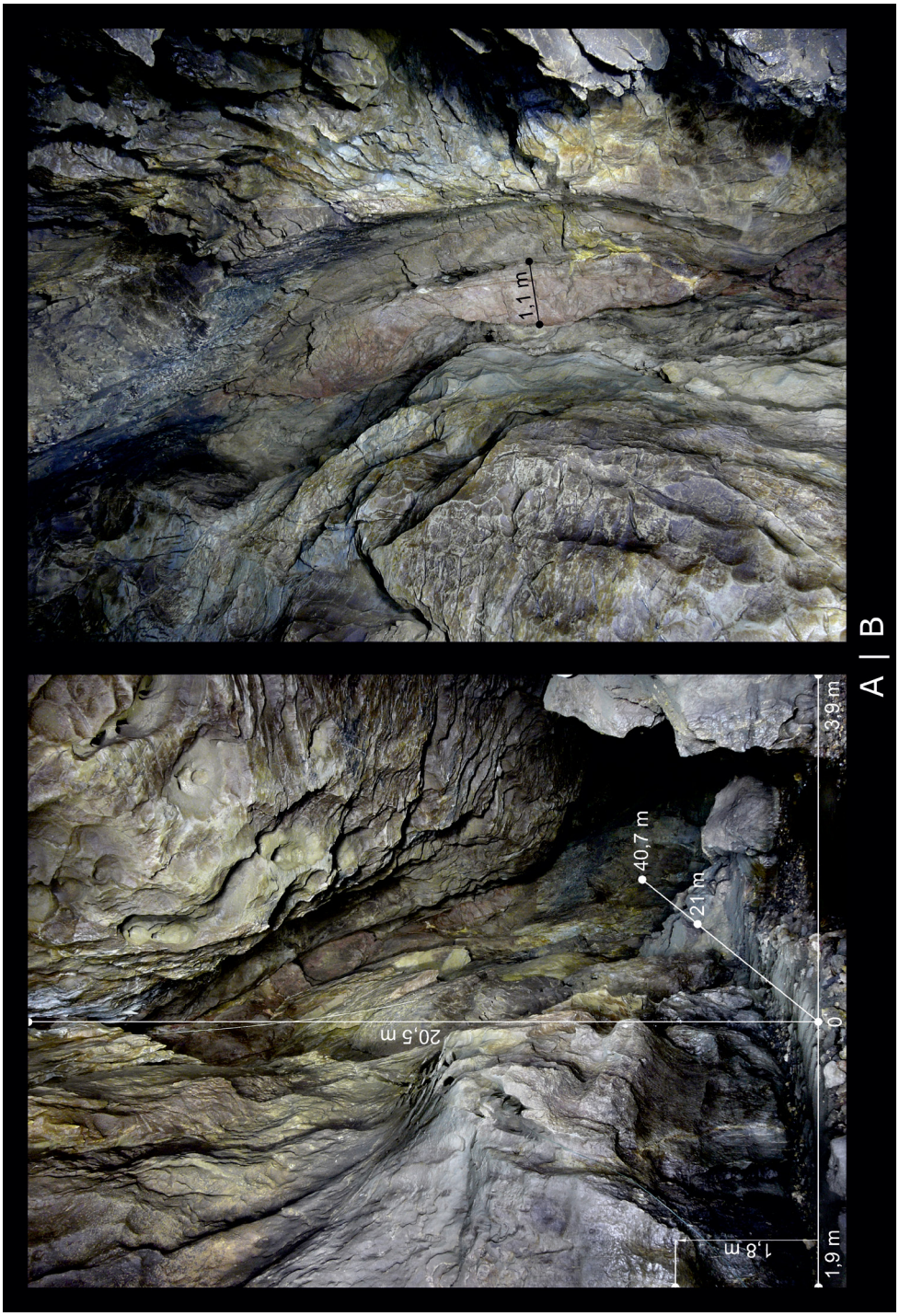


Fig. 11. Calcite breccia w/red-brown clays and loess loam: A: SE fault in NBR (max. thickness 3.5 m); B: detail of A (ceiling).

In places, calcite fills contain varicolored intergranular clayey inclusions and/or clayey zones. Clayey zones are parallel to the host fracture faces and are 0.5–5 mm thick. In type A they alternate with growth zones of the calcite and show degrees of calcification. In type B, clayey zones occur only at contact of the deposit with the limestone or calcite A and are intensely calcified (Gregor 1976; Gregor & Princ 1977; Pelíšek 1980). Such clays also fill space between calcite fragments in calcite breccias (Figs 11, 12).

Geochemical signatures indicate that the red to wine red but also greenish and bluish clays are sediments of the Rudice Formation. The Rudice clays and silts, as well as most of the Fe-mineralization, could have been emplaced during Saxon tectonic movements in the Lower Cretaceous period of intense tropical weathering and vertical karstification, and also during later fault movements. The circulation of Fe-enriched natural waters and deposition of limonitic-hematitic Fe-ores was characteristic of the evolution of paleokarst of the Rudice, Moravian Karst type (Burkhardt 1974; Burkhardt *et al*. 1975; Bosák 1980; Dvořák *et al*. 1993). Red-brown terra rossa clays (Paleogene to Pleistocene in age) were emplaced later, probably during Alpine (Alpine-Carpathian) and neotectonic fault activity.

Ocher-yellow, yellowish-brown and grayish-brown zones in primary calcites and intergranular (interfragmental) fills in calcite breccias are formed by loess loam. Loess in the Moravian Karst is Pleistocene, more specifically Würm in age and thus, its presence is considered an indication of Pleistocene, particularly Late Pleistocene movements. Locally, the host calcite or calcite breccia contain type A11 calcite (Tab. 1). Type A11 characteristically displays bright yellow UV fluorescence – a phenomenon that is believed to be due to the presence of organic acids (Gregor 1976). This observation indicates that these deposits might have originated from cold solutions descending from the surface. The presence of organic matter in some A11 fills supports this notion.

Coarse crystalline, light honey-colored secondary calcite – freshwater sinter of generation I – (G–I in Tab. 1; in the Moravian Karst, Gregor (unpublished manuscript) recognizes six basic generations of calcite speleothems) was found in some karstified fractures, in one case adjacent to an A11 fill. This shows that the deposition of calcium carbonate might have shifted from primary to secondary calcite.

Large-scale fractures, particularly those that reach the surface, serve as conduits of descending meteoric waters and thus, are karstified. Various sinterforms, typically stalactitic (wall) flowstones, issue from these features. Fragments of such sinterforms were found in brecciated fills of several faults, namely those in the Giant Dome (GnD), Sandy Dome (Písčitý dóm), the Gothic Dome (GtD) fault, and the SE fault in the New Bull Rock Cave (Gregor 2013, 2014b). In the Tipeček Gallery (Figs 2 and 9; Burkhardt *et al*. 1975; Gregor 2015), tectonic slickensides were discovered on a large sinterfall (wall flowstone), at the contact of the formation with the limestone rock along a fracture zone 160°/80° SW. Considered together, these facts represent strong evidence of neotectonic, Quaternary reactivation of these fractures.

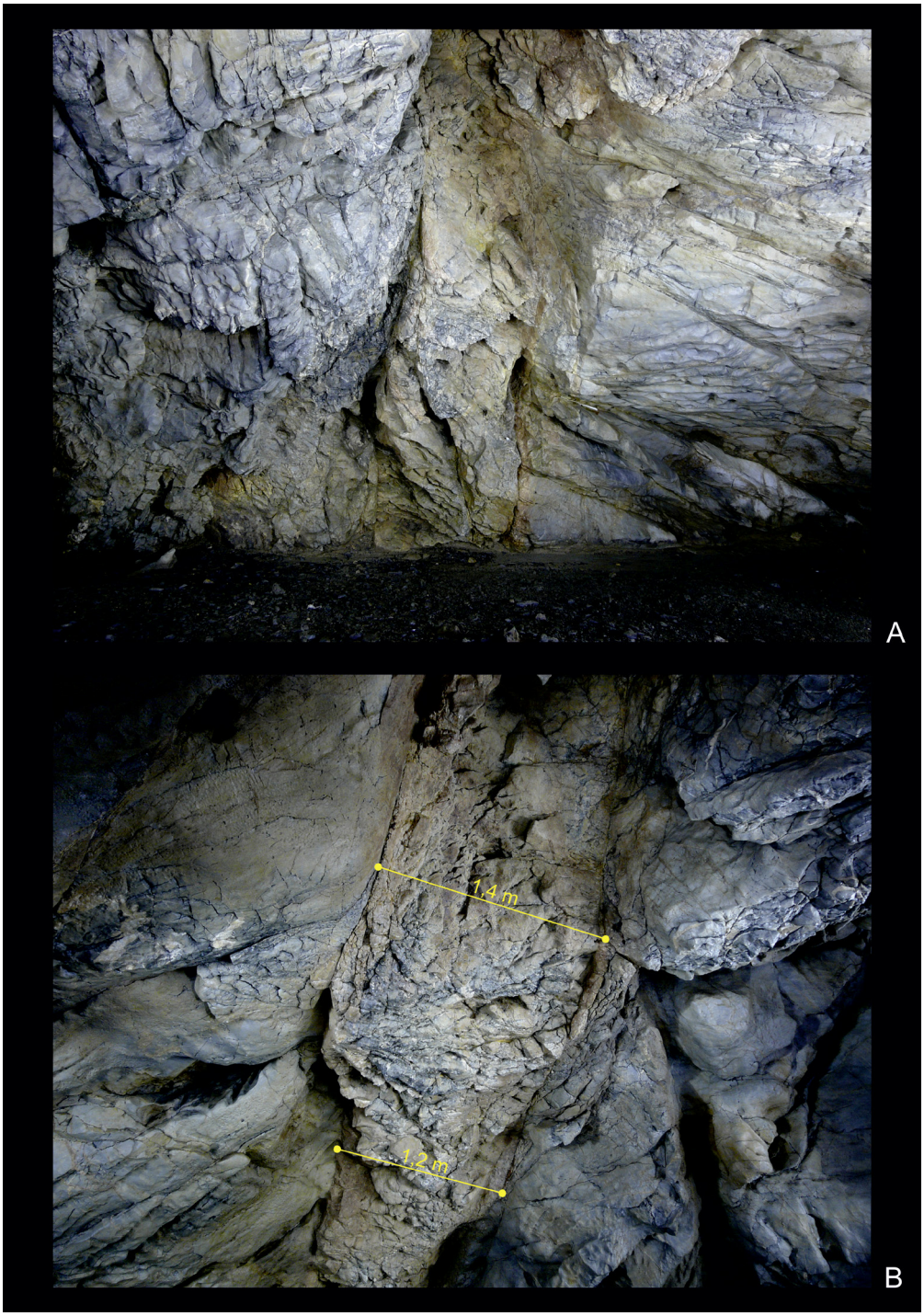


Fig. 12. Calcite breccia w/red-brown clays and loess loam: A: Tablets fault (max. thickness 1.5 m); B: detail of A (is taken from the opposite direction).

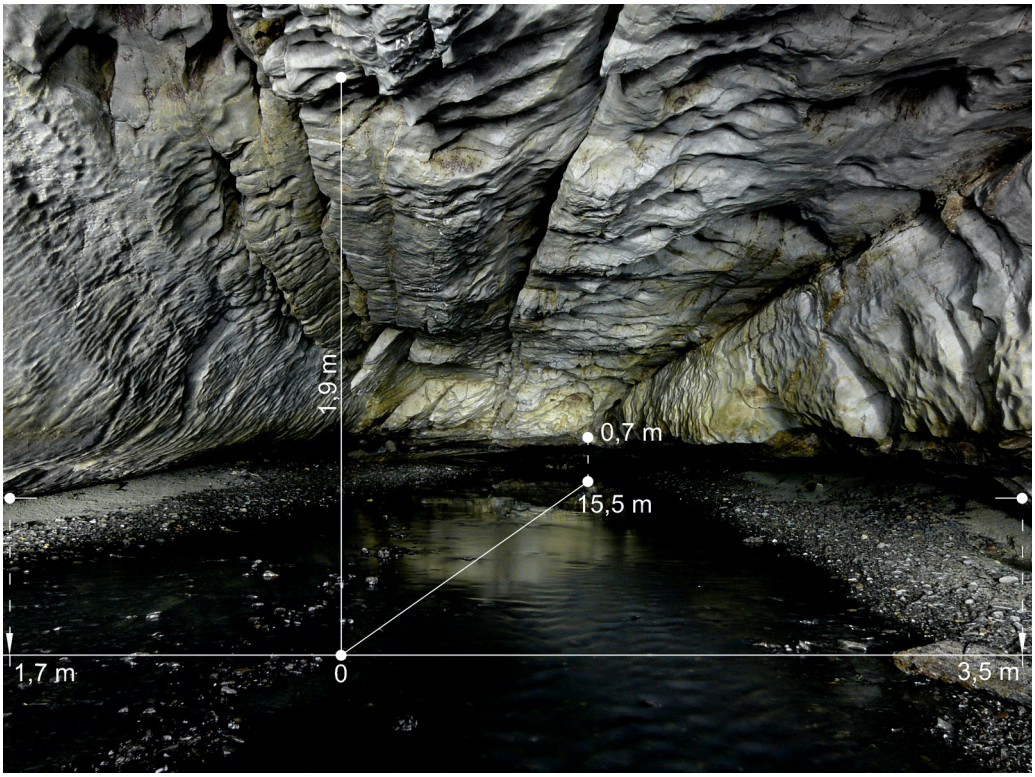


Fig. 13. Giant Dome semi-siphon and low passage: upstream view from the Sandy Dome. The flat ceiling of the semi-siphon (in the background) is leveled across strata dipping 35–40° NW.

Note: The age of calcite speleothems in the Moravian Karst caves ranges from the Middle Pleistocene to the present (Tab. 2; also Musil *et al*. 2018). The oldest age data obtained so far, using the $^{230}Th/^{234}U$ method, are from a relic of floor sinter from the Holštejnská Cave. The middle layer is 230 ka, δ +32/−44 ka old. The bottom layer exceeds 350 ka in radiometric age and, according to paleomagnetic data, could be more than 780 ka old (Hercman *et al*. 1997; Kadlec *et al*. 1999, 2001). Large sinterfalls (wall flowstones) such as that in the Tipeček Gallery, belong to Generation III (interstadial W2/W3) to VI (Recent, Tab. 2).

Flat-roofed sections of the Rudice Swallow Hole and Bull Rock caves

In the Rudice Swallow Hole Cave, typical flat-roofed sections include the Giant Dome semi-siphon, the Black Loams semi-siphon, and the three semi-siphons, SS1 to SS3, in the Easter Cave.

The 180 m long Giant Dome-Sandy Dome section with the 70 m long Giant Dome semi-siphon (Figs 2, 9, 13, and 14) and the following low-profile tunnel passage is

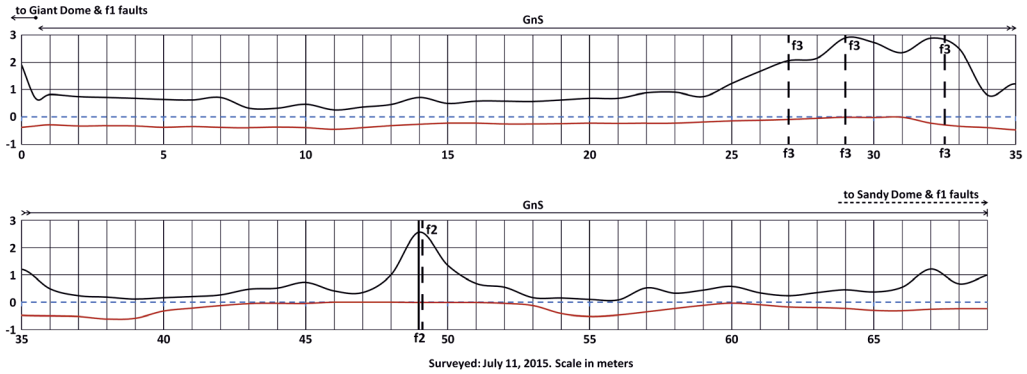
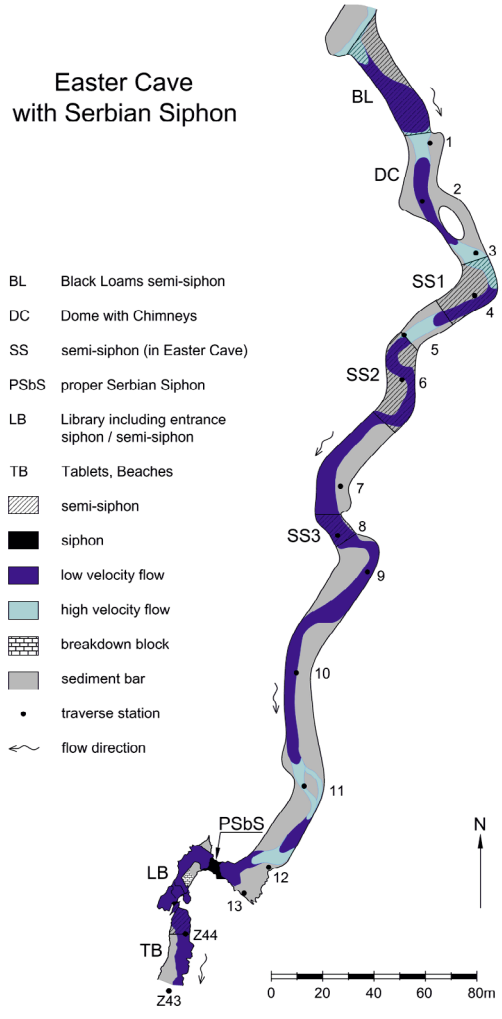


Fig. 14. Giant Dome semi-siphon, longitudinal XS; f1, f2, f3 – see Fig. 16.



bounded by a 160°/80° SW fault in the Giant Dome, and intersecting faults 160°/80° SW and 135°/80° NE in the Sandy Dome (Fig. 9). Brecciated fills of these faults contain more than one generation of primary calcite as well as Rudice clays and loess loam (Gregor & Princ 1977) and two of them also fragments of secondary calcite.

The Serbian Siphon is the conventional dividing point between the Rudice Swallow Hole Cave and the Bull Rock Cave (Fig. 2; Gregor *et al*. 2014; Havlík & Mikeš 2016). The 6 m long and 2 m deep siphon represents the deepest structural low in a *ca*. 450 m long, tectonically lowered section of the tunnel passage (Figs 15 and 16). The section, abbreviated as BEL, extends from the Black Loams semi-siphon on the Rudice side (Figs 17

Fig. 15. BEL section, ground plan. Explanatory notes are included in the map. A compilation of surveys by D. Hypr, P. Čížek, A. Nejezchleb, V. A. Gregor, J. Havlík & D. Mikeš (see also Burkhardt *et al.* 1975; Hypr 1976; and Havlík & Mikeš 2016). For a detailed geologic map of EC see Gregor (2015).

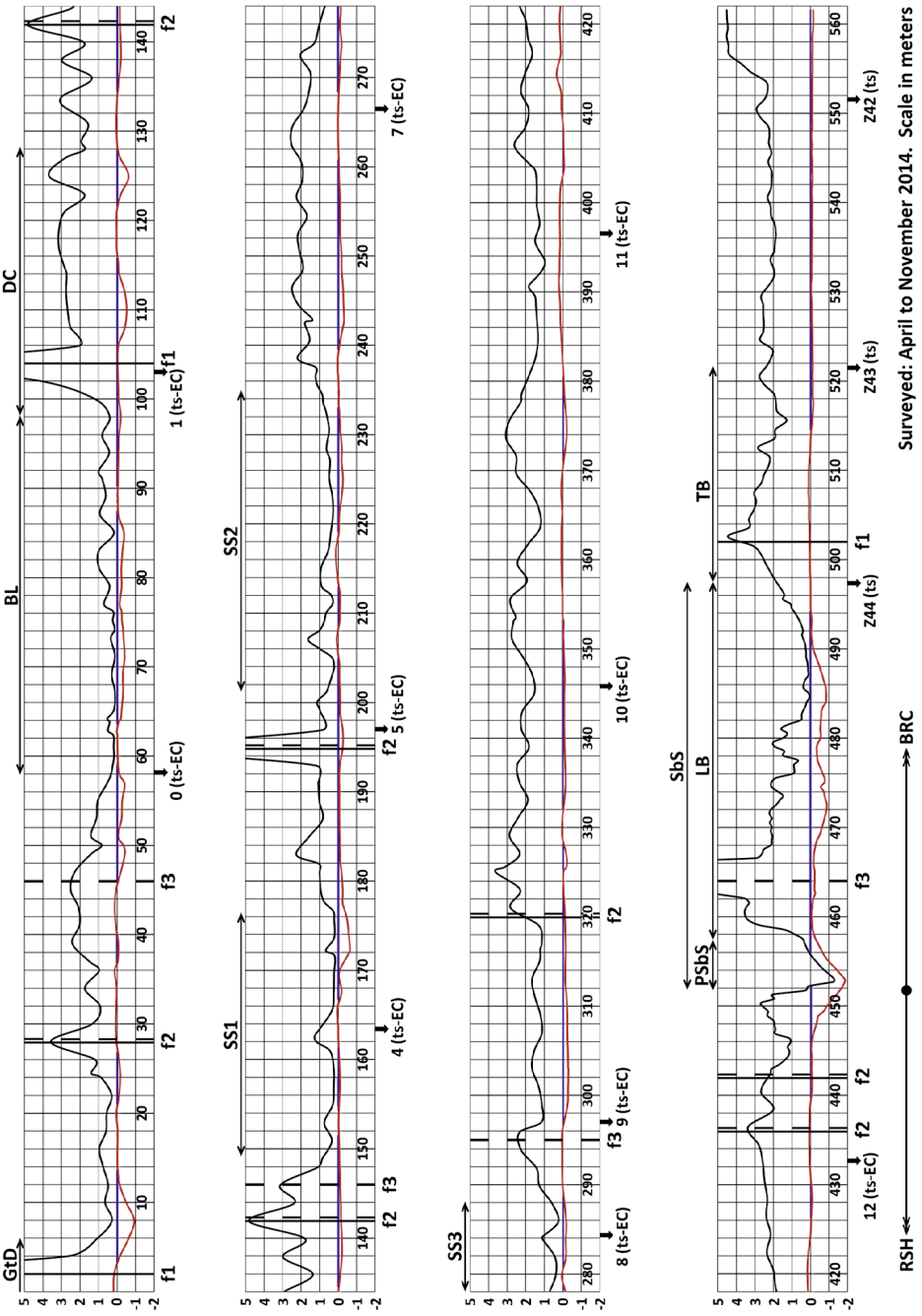


Fig. 16. BEL section, longitudinal XS. Explanatory notes: f1 (bold solid line) – fault w/neotectonic AVD ≥ 2 m; f2 (parallel solid and dashed line) – fault or fault zone w/neotectonic AVD < 2 m; f3 (dashed line) – joint or joint zone w/no AVD; (ts) – traverse stations w/ID.

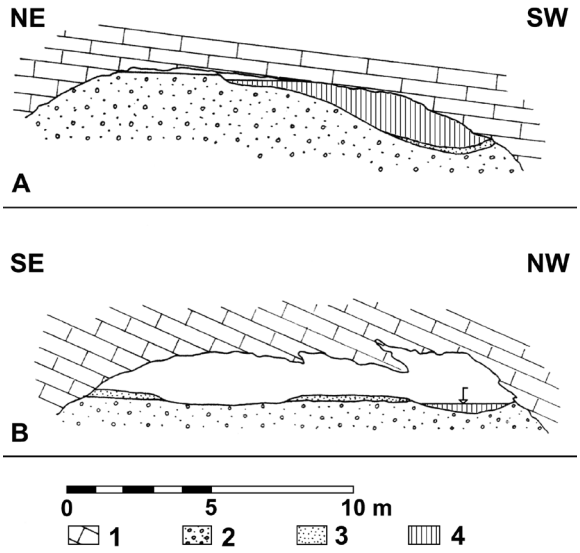


Fig. 17. Transverse XS of the Black Loams semi-siphon (A) and the Easter Cave (B). Explanatory notes: 1 – limestone rock; 2 – fluvial sediment, sandy gravel; 3 – fluvial sediment, sand and clay; 4 – water body (Jedovnice Creek). From Hypr (1976) (used with permission).

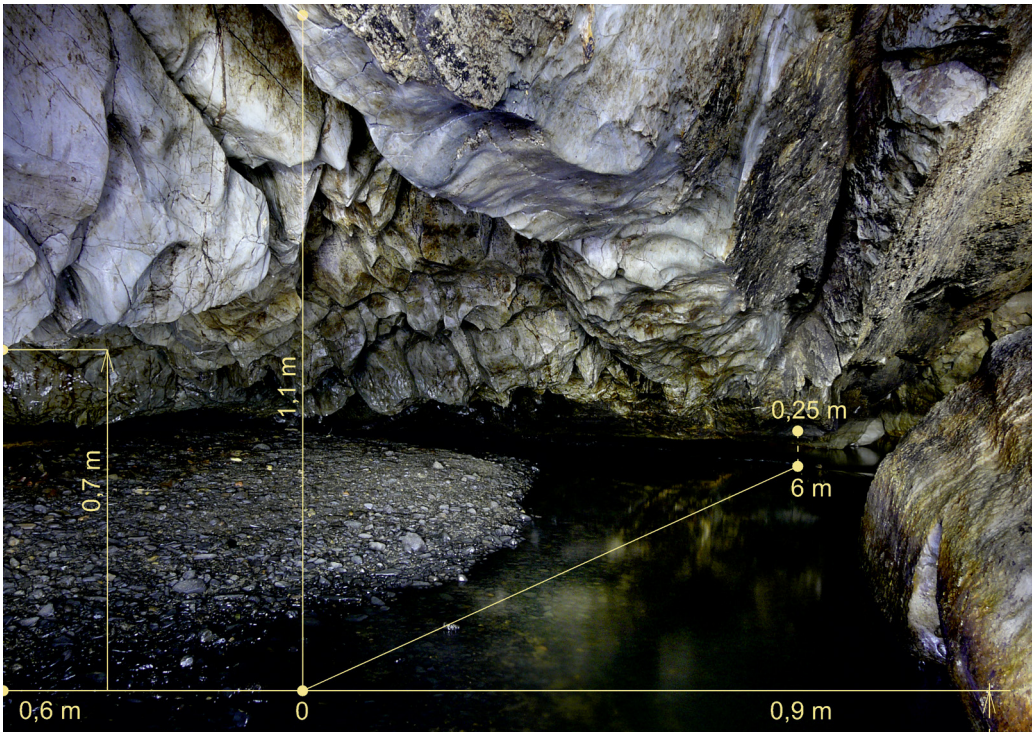
and 18) to the Tablets on the Bull Rock side (Fig. 19). It includes the 40 m long semi-siphon, the proper Easter Cave (350 m), and the 40 m long Library. The Library is part of the Serbian Siphon – a chamber between the actual siphon and the semi-siphon at the Tablets, the Peek (Jukadlo, Fig. 15).

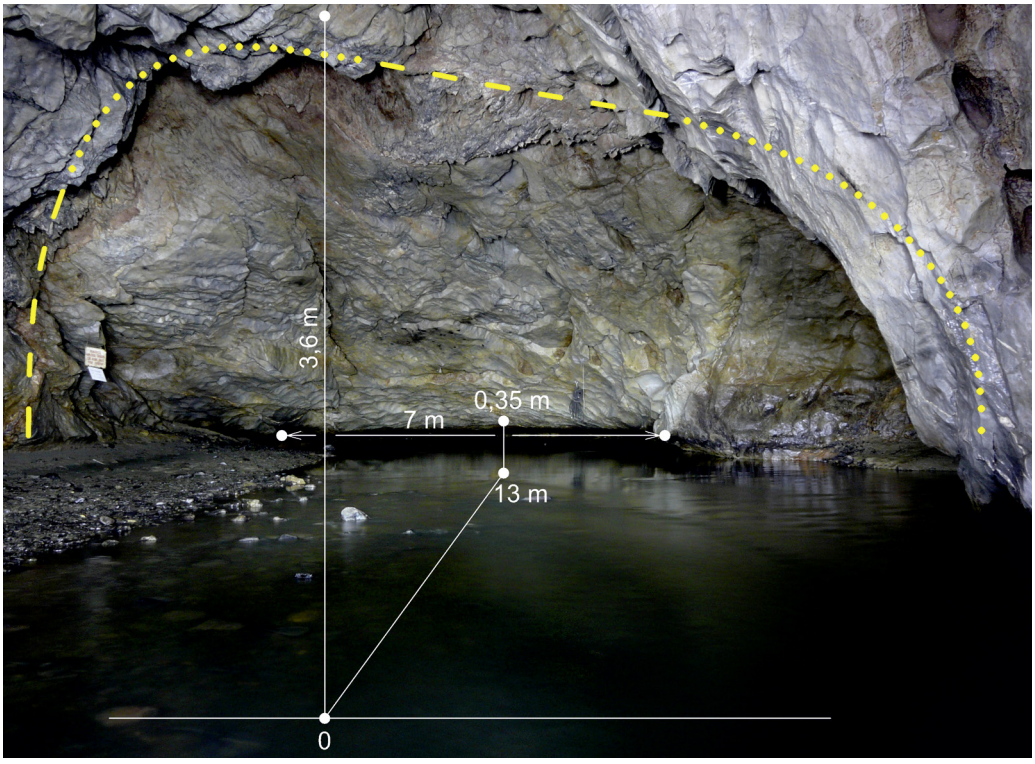
The BEL section, as a whole, is bounded by faults with calcite breccia: at the northern end, in the Gothic Dome, by transecting faults 160°/80° SW (also with sinter fragments) and 140°/60° NE (Fig. 20); and, in the south, by a W-E fault 86°/80° N at the Tablets (Fig. 21). At the latter point, the passage regains its original tunnel form (Fig. 15). All of the mentioned faults contain calcite-limestone breccia with at least two generations of calcite cement, Fe-mineralization, and red-brown and ocher-yellow clays (Fig. 12). Within the section, additional faults limit some of the flat-roofed blocks – *e. g.* the 160°/80° SW and 132°/80° NE faults in the Dome with Chimneys that terminate the southern end of the Black Loams semi-siphon as well as the northern end of the semi-siphon SS1.

At a normal water level (corresponding to an average flow rate of 0.15 $m^3.s^{-1}$ or, in other words, to the 330-daily flow) the proper Easter Cave is throttled by three flat-roofed semi-siphons, SS1 to SS3 (Figs 15, 16, and 22). At higher water levels (flow rates) the

Fig. 18. Black Loams semi-siphon, entrance from the Gothic Dome (in the background, downstream view). Karstification in the front part is controlled by joints *bc*. ▶

Fig. 19. Tablets, upstream view. The flat ceiling in the background (the Peek ss) is 0.35 m high; it is leveled across strata dipping 30–35º to the SE. The flat-roofed section abruptly transits into the tunnel passage in front. The sunken block with the semi-siphon is separated from the tunnel passage by the Tablets fault. The yellow dashed line (dotted behind the coulisses) schematizes the course of the fault.


1,1 m
0,7 m
0,25 m
6 m
0,6 m
0
0,9 m


3,6 m
7 m
0,35 m
13 m
0

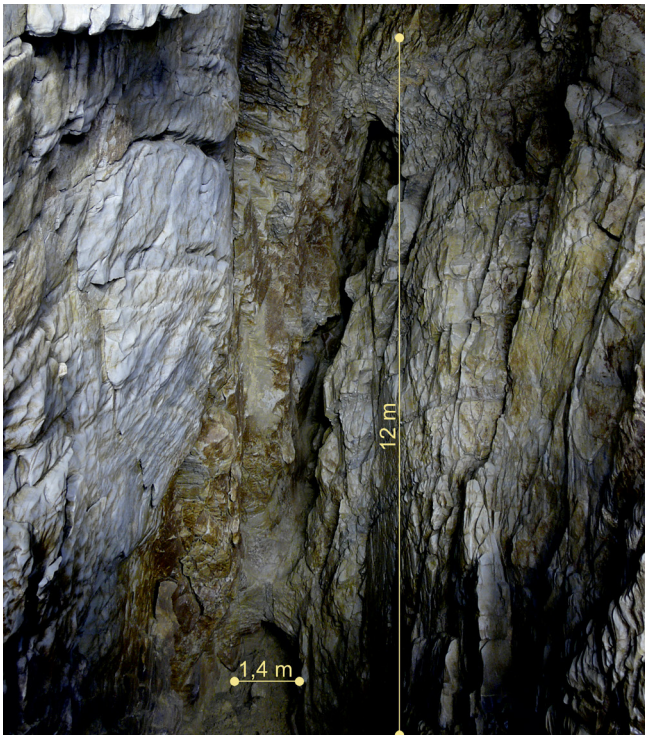


Fig. 20. Gothic Dome fault 160°/80° SW.

▼ Fig. 21. Tablets fault 86°/80° N.



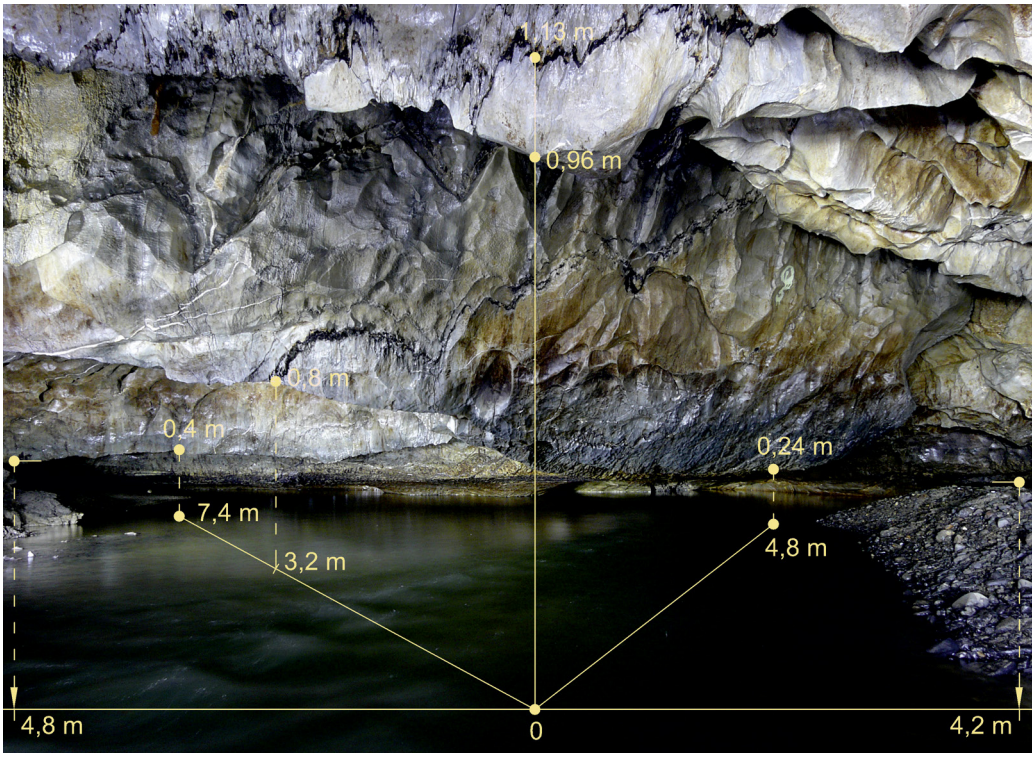


Fig. 22. Easter Cave, semi-siphon SS2, downstream view.

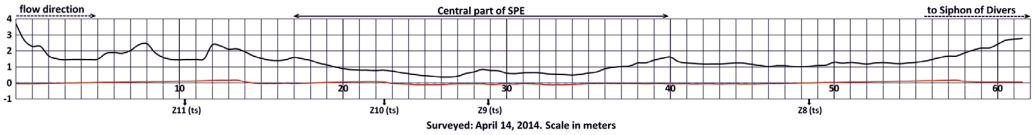


Fig. 23. Stretch of Preliminary End, longitudinal XS. The proper semi-siphon extends between 17 m and 40 m on the horizontal (*x*) scale; (ts)-traverse stations and ID.

semi-siphons become siphons. During high floods (≥ 9.5 m^3.s^{-1}, water level ≥ 6 m above normal, flood flow through the Old Bull Rock Cave), the entire BEL section, except for the 20+ m high Dome with Chimneys, is transformed into practically one long siphon (BURKHARDT *et al*. 1975; GREGOR *et al*. 2014).

In the Bull Rock Cave, flat-roofed sections are represented by the Peek semi-siphon of the Library (Fig. 19), the Stretch of the Preliminary End (SPE, Figs 23 and 24), and the semi-siphon in the Broken-in Rock Cave (Figs 25 and 26), all of them in the main passage. Flat-roofed sections are also found in the geologically younger phreatic water passage, the water channel Canyons (Kaňony, Fig. 27).



Fig. 24. Higher part of the Stretch of Preliminary End (upstream view) w/tabular ceiling and a roof half-tube, remodeled by later erosion.

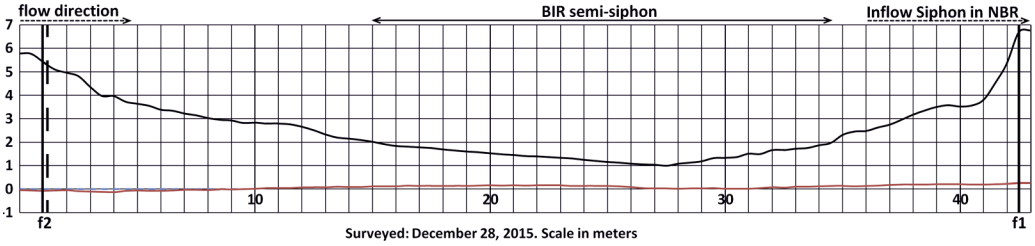
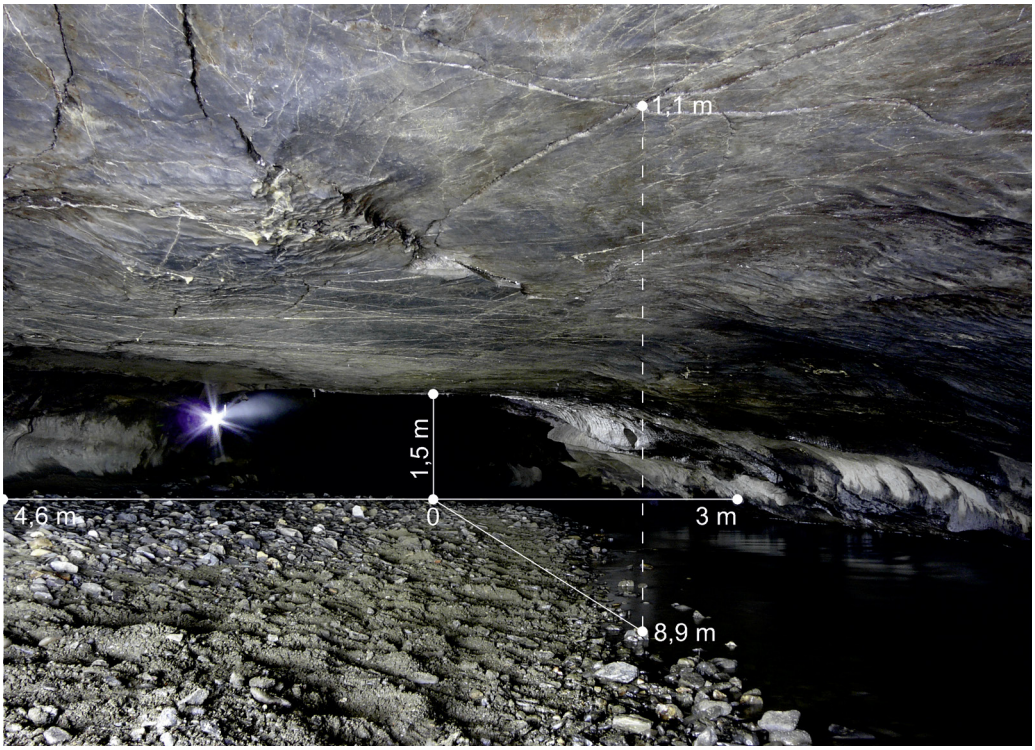


Fig. 25. BIR semi-siphon, longitudinal XS; f1, f2 – see Fig. 16.

Fig. 26. BIR semi-siphon, upstream view. ▶

Fig. 27. Flat-roofed section in the Canyons (NBR), upstream view.


1,1 m
1,5 m
4,6 m
0
3 m
8,9 m


0,6 m
0,6 m
10 m
0,6 m
0
2,1 m

Origin of flat-roofed sections and paragenesis

Flat-roofed sections are found in tectonically sunken blocks; these blocks are associated with faults that have a history of repeated movements. Typical examples include the BEL section between the Gothic Dome and the Tablets, and the Giant Dome semi-siphon with the low passage between the Giant and Sandy domes.

The sinking is post-genetic with respect to the main passage. Since the passage is Pleistocene in age, the sinking is a result of neotectonic, particularly Pleistocene to Holocene movements. Within the sunken blocks, the passage was lowered, filled with sediment, and the lowest parts of the original ceiling (in some cases bounded by additional normal faults) were brought down into contact with the water body and thus, exposed to the effects of antigravitational corrosion – so called paragenesis (Fig. 28). Subsequent sediment deposition has led to the reduction of the convacuation space and further upward corrosion.

The terms "paragenesis" and "paragenetic" – "birthing beside" and "born beside", respectively – mean, in principle, the origin of two different entities at their mutual contact so that one influences the formation of the other. In geology, paragenesis is usually applied to a characteristic association or occurrence of minerals or mineral assemblages in ore deposits, connoting contemporaneous formation. In other words, it means an equilibrium sequence of mineral phases. In speleology, paragenesis, also known as antigravitational or antigravitative erosion (Pasini 2009), is the upward dissolution of the ceiling in a water filled cave passage due to a protecting (armoring) sediment cover of the underlying floor.

According to Renault (1968, 1970) and others (Ford & Williams 1989, 2007; Ford 2000; Lauritzen & Lundberg 2000; Farrant & Smart 2011; Lauritzen 2013), paragenetic passages originate by enlargement of water table or phreatic cave passages. With enlargement, flow velocity may be reduced, permitting deposition of fluvial sediment that protects the floor and lower walls so that solution proceeds upwards, to the ceiling, on a thickening column of sedimentary fill (Ford & Williams 1989, 2007). As a result, the ceiling (cave roof) recedes – rises. The vertical amplitude of such paragenesis can exceed 50 m. Remarkably flat ceilings can be leveled across dipping strata.

Burkhardt *et al*. (1975), Ford & Williams (1989, 2007) and Farrant & Smart (2011) allege that flat (tabular) ceilings are the primary and most important characteristic of paragenetic caves. In the Jedovnice Creek cave system, the tabular ceilings are horizontal or nearly horizontal; they are leveled across beds with a dip as high as 45° as well as steeply slanting fractures and almost vertical morphostructures (Figs 19 and 29).

The occurrence of other paragenetic features – such as ceiling half-tubes and anastomoses, pendants and drainage grooves – depends on a number of factors. These include the petrographic and chemical composition of the limestone rock and its structural setting, the character and velocity of the flow, and the character and configuration of the sedimentary fill. Since the morphology of the Jedovnice Creek caves is strongly controlled

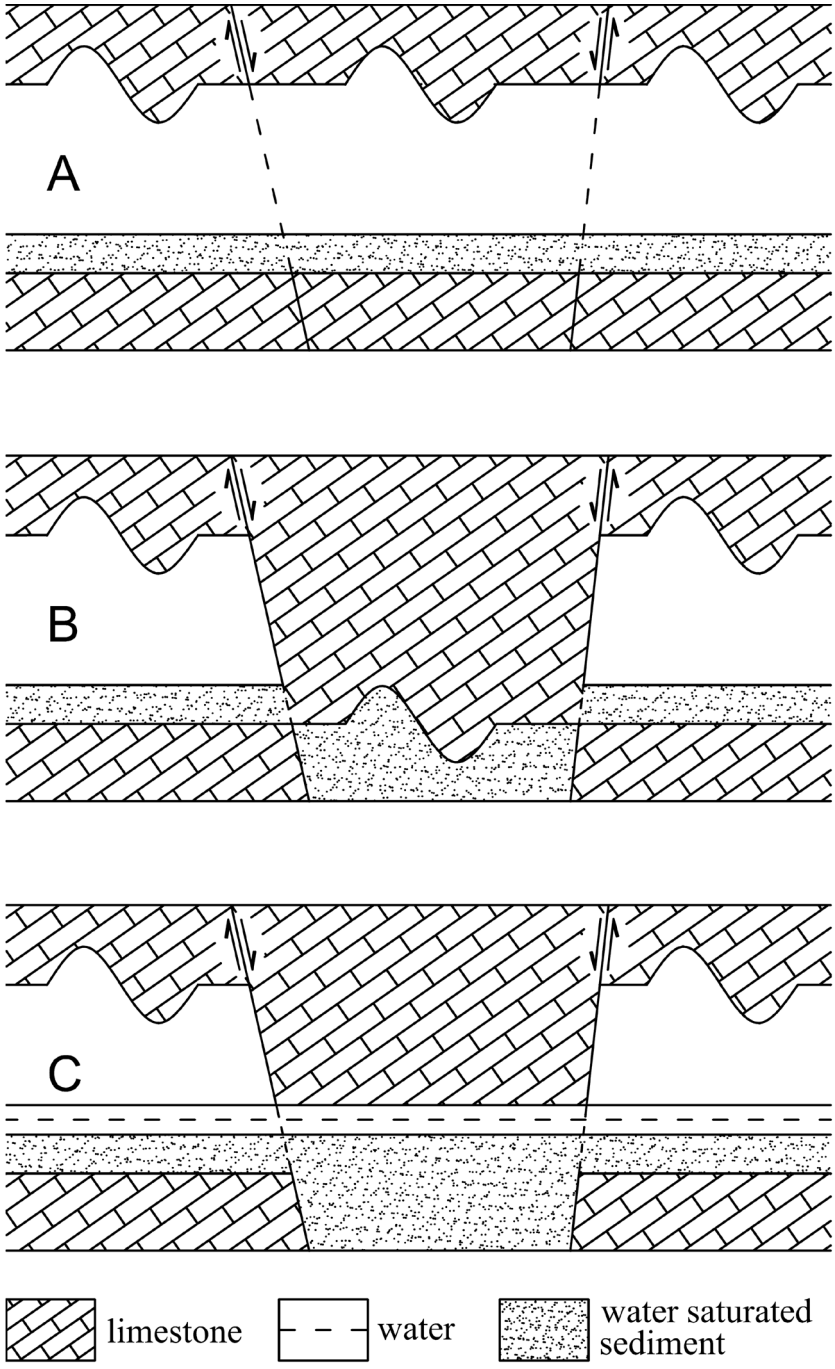


Fig. 28. Basic stages of the development of flat-roofed sections by normal faulting and paragenesis, schematic model. A: cave passage and faults in the limestone strata; B: neotectonic sinking of a limestone block: the ceiling is brought into contact with water- saturated sediment; C: sunken ceiling in contact w/flowing water (proper antigravitational corrosion).

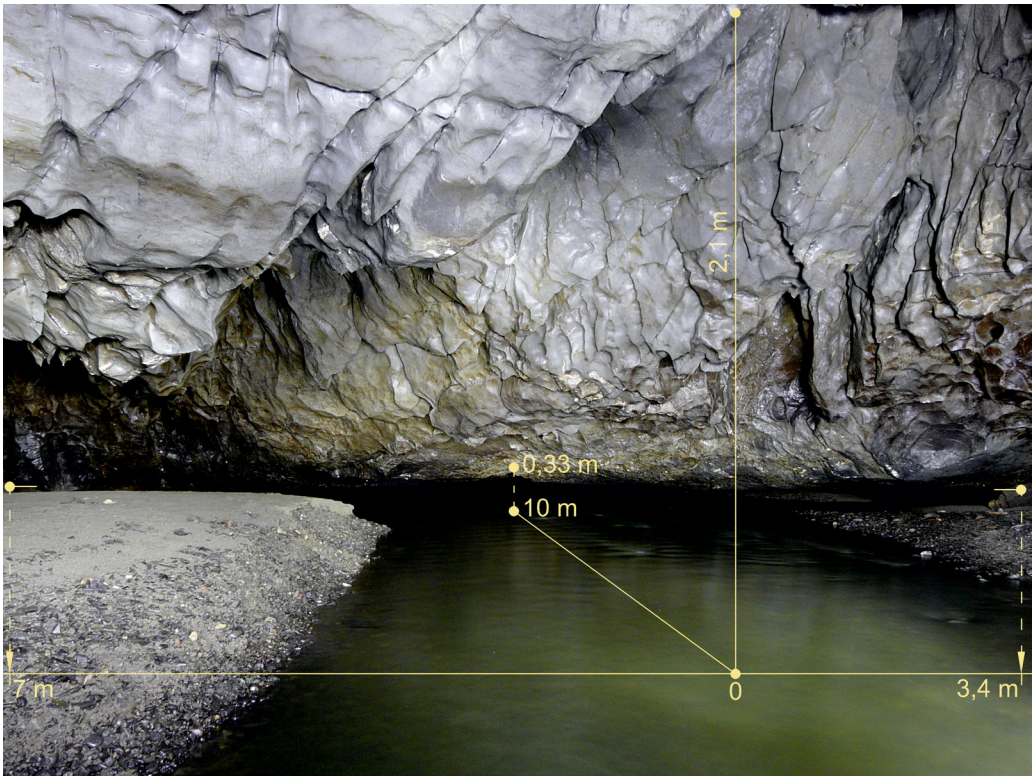


Fig. 29. Easter Cave, semi-siphon SS1, downstream view. An example of flat ceiling generated in steeply inclined strata.

by linear structural elements, curved (winding) features such as anastomoses are absent; both wall and ceiling features tend to be linear, the latter including linear half-tubes, linear drainage grooves and linearly arranged shallow pockets.

The planarization of the ceilings removed positive relief, but preserved some negative relief such as inverse solution pots, segments of deeply karstified joints and, in places, the mouths of vertical karst conduits. The selective nature of the corrosion is illustrated by petromorphs of calcite veins and vein meshes that stand in relief from the limestone mass (Fig. 26).

The superimposed, present-day morphology includes a variety of erosional and solutional features. The most obvious are wall and ceiling scallops (Fig. 30). These forms fall into two size categories. Small scallops (3–9 cm in length) are less abundant than large scallops (15–40 cm long). Morphometric analyses of these features, using formulas by Bögli (1980) and Ford & Williams (1989), yielded flow velocities as high as 2 $m.s^{-1}$ and flow rates up to 12 $m^3.s^{-1}$ for the small sculptures, thus data higher than, or equal to, recent high flood flow rates and velocities. Large scallops formed at much lower velocities and flow rates – lower than 1 $m.s^{-1}$ and 2.5 $m^3.s^{-1}$, respectively. The presence

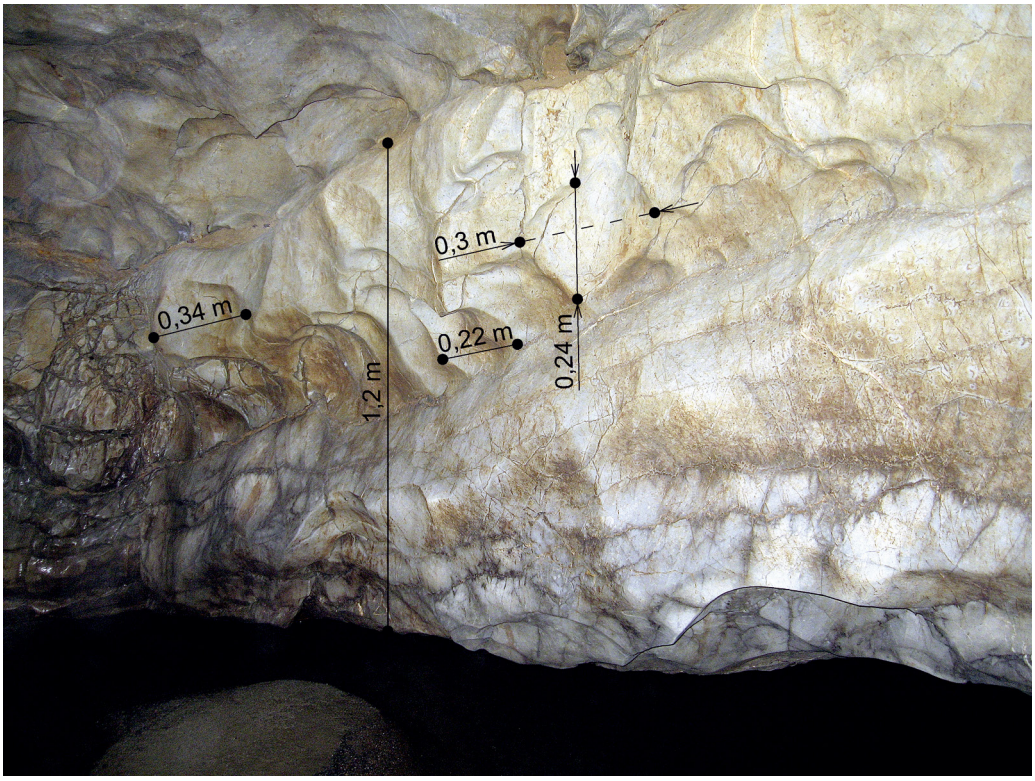


Fig. 30. Scallops in the Library, downstream view.

of ceiling scallops can be attributed to a relatively small cross-section – *ca*. 13 m^2 – the entire perimeter of which is wetted by a turbulent flow (stream). The orientation of scallops follows the present-day flow direction of the Jedovnice Creek.

Fractures that serve as conduits of atmospheric (autogenic) water also discharge into the paragenetic sections. As a result, the present-day morphology includes further development of negative relief, chiefly the formation of inverse ceiling pots – diffusion corrosion pots (sensu FRANKE 1963) rather than mixing corrosion pots (sensu BÖGLI 1964, 1980) – as well as that of chimney-like cavities.

Conclusions

Low-profile, flat-roofed sections of the main, generally tunnel-shaped and rugged passage of the Jedovnice Creek cave system are primarily of tectonic origin. They are post-genetic with respect to the tunnel form. Normal faulting along neotectonically (Pleistocene to Holocene) reactivated Saxon-Alpine and Variscan faults resulted in the sinking of limestone blocks and thus, lowering the ceiling of the passage by < 2 to 4 m and bringing it into contact with the water body – the stream. As a result, the ceiling was (and continues

to be) exposed to antigravitational corrosion (paragenesis) and remodeled, the major features being flat, tabular roofs. Such roofs are generated even in steeply inclined strata. Locally the flat-roofed sections exhibit secondary paragenetic morphoforms, *e. g.*, linear ceiling half-tubes and grooves. The superimposed, present-day morphology includes a variety of erosional and solutional (corrosional) features – typically scallops.

Three main development phases of paragenetic sections can be recognized:

(1) Tectonic sinking of limestone blocks and thus, lowering segments of the tunnel passage. Originally, the passage was ≥ 2 m high.

(2) Leveling of the original roof at water contact, formation of horizontal, tabular ceilings in both subhorizontal (2º to 10º) and moderate (20º to 45º) bedding dips.

(3) Superimposition of the present morphology, mainly scallops. Vertical influx of atmospheric water from joints and breakdown also contributed to the current shape of these sections.

Acknowledgments

The manuscript benefited from reviews by Marta N. Gregor, B. A., Dr. Jaroslav Kadlec, Dr. Andreas Kroh, Dr. Alexander Lačný, CSc., Univ. Prof. Dr. Rudolf Musil, DrSc., Dr. Lukas Plan, and Dr. Peter R. Thompson. Special thanks are extended to Dr. Květoslava Havlíková for her technical and moral support.

References

Bábek, O., Briestenský, M., Přecechtělová, G., Štěpančíková, P., Hellstrom, J.C. & Drysdale, R.N. (2015): Pleistocene speleothem fracturing in the foreland of the Western Carpathians: a case study from the seismically active eastern margin of the Bohemian Massif. – Geological Quarterly, **59**/3: 491–506.

Becker, A. (1993): An attempt to define a "neotectonic period" for central and northern Europe. – International Journal of Earth Sciences, Geologische Rundschau, **82**/1: 67–83.

Bosák, P. (1980): Spodnokřídový fosilní kras plošiny v Moravském krasu. – Československý kras, **31**: 57–67.

Bögli, A. (1964): Érosion par melange des eaux (Mixed-water corrosion). – International Journal of Speleology, **1**: 90–99.

Bögli, A. (1980): Karst hydrology and physical speleology. – 284 pp., Berlin, Heidelberg, New York (Springer-Verlag).

Burkhardt, R. (1973): Geologische Verhältnisse der Höhle Býčí skála. – Acta Musei Moraviae, Sci. naturales, **56–57**: 57–74.

Burkhardt, R. (1974): Rudická plošina v Moravském krasu – část I. Příspěvek k teorii fossilního krasu a geologickému vývoji. – Acta Musei Moraviae, Sci. naturales, **59**: 37–58.

Burkhardt, R., Gregor, V.A. & Hypr, D. (1975): Rudická plošina v Moravském krasu – část II. Geologická stavba a vývoj Rudického propadání. – Acta Musei Moraviae, Sci. naturales, **60**: 87–124.

Burkhardt, R., Gregor, V.A. & Hypr, D. (1977): Speleologický a geologický charakter Rudického propadání. – Sborník Okresního vlastivědného musea v Blansku, **6–7**: 101–110.

Dudek, A. (1980): The crystalline basement block of the Outer Carpathians in Moravia: Brunovistulicum. – Rozpravy Československé akademie věd, řada matematických a přírodních věd**, 90**/8: 3–85.

Dvořák, J., Štelcl, O., Demek, J. & Musil, R. (1993): Geologie a geomorfologie Moravského krasu. – In: Musil, R. (ed.): Moravský kras labyrinty poznání. – pp. 31–75, Adamov (Jaromír Bližňák GEO program).

Dvořák, J. (1994): Neogenní výplň údolí u Jedovnic a otázka stáří hlavních jeskynních úrovní v severní části Moravského krasu. – Journal of the Czech Geological Society, **39**/2–3: 235–240.

Farrant, A.R. & Smart, P.L. (2011): Role of sediment in speleogenesis; sedimentation and paragenesis. – Geomorphology, **134/**1–2: 79–93.

Ford, D.C. (2000): Speleogenesis under unconfined settings. – In: Klimchouk, A.B., Ford, D.C., Palmer, A.N. & Dreybrodt, W. (eds): Speleogenesis: Evolution of karst aquifers. – pp. 319–324, Huntsville (National Speleological Society).

Ford, D.C. & Williams, P.W. (1989): Karst geomorphology and hydrology. – 601 pp., London (Unwin Hyman).

Ford, D.C. & Williams, P.W. (2007): Karst Hydrogeology and Geomorphology. – 562 pp., West Sussex (John Wiley & Sons Ltd.).

Franke, H.W. (1963): Formgesetze der Korrosion. – Das Laubensteingebiet im Chiemgau: seine Landschaft, seine Höhlen und Karsterscheinungen. – Jahreshefte für Karst und Höhlenkunde, **18**/3: 207–224.

Gregor, V.A. (1975): Beitrag zur Methodik einer Gesamtuntersuchung der sekundären Mineralausfüllung und der physikalisch-chemischen Parameter des Höhlenmilieus im Mährischen Karst (CSSR). – Annales de Spéléologie, **30**/4: 691–694.

Gregor, V.A. (1976): Geometrie a relativní chronologie puklinových zón a zlomů v Moravském krasu. Geometry and relative chronology of joint zones and faults in the Moravian Karst. – Moravian Museum, Institute of Geology, Department of Karst Research. Open File Report KOMM, **22**: 1–63.

Gregor, V.A. (1981): Geological development and age of the caves in the Moravian Karst (Czechoslovakia). – In: Beck, B.F. (ed.): Proceedings of the 8th International Congress of Speleology. – pp. 808–809, Bowling Green (Georgia Southwestern College).

Gregor, V.A. (1986): Vertical hydrodynamic zoning in carbonate rocks. – Hydrological Science and Technology, **2**/1: 33–38.

Gregor, V.A. (2013): Nová Býčí skála a Stará štola – pohled do nitra aktivního zlomu. – Sborník Muzea Blansko, **2012**/1: 12–29.

Gregor, V.A. (2014a) Komíny a vyšší jeskynní patra v Rudickém propadáni, Moravský kras. – Sborník Muzea Blansko, **2013**/1: 51–70

Gregor, V.A. (2014b): Komíny a vyšší jeskynní patra v Nové Býčí skále, Moravský kras. – Sborník Muzea Blansko, **2013**/1: 32–51.

Gregor, V.A. (2015): The Moravian Karst. The Jedovnice Creek cave system of the Rudice Plateau in the Moravian Karst – the Rudice Swallow Hole, Bull Rock and Bar caves. – Available online at www.byciskala.cz/MaRS/index.php?show=clanek&id=554; last accessed 19.7.2015.

Gregor, V.A., Havlík, J. & Mikeš, D. (2014): Srbský sifon – konec Rudického propadání a počátek Býčí skály. – Sborník Speleoforum, **33**: 16–22.

Gregor, V.A. & Princ, M. (1975a): Die Radiotest-Methode und ihre Anwendung in der geologishen Forshung von Karstgebieten. – Annales de Spéléologie, **30**/4: 681–690.

Gregor, V.A. & Princ, M. (1975b): Untersuchungen über Typen, Morphologie, Genesis und physikalisch-chemische Eigenschaften der sekundären Kalzitformen in Höhlen des Mährischen Karste. – Annales de Spéléologie, **30**/4: 673–680.

Gregor, V.A. & Princ, M. (1976): Radiotestová metoda a její aplikace ve speleologickém a geologickém výzkumu krasových oblastí. – Acta Musei Moraviae, Sci. naturales, **61**: 53–96.

Gregor, V.A. & Princ, M. (1977): Výzkum sekundární minerální výplně a fyzikálně-chemických parametrů prostředí jeskyní v Moravském krasu. – Sborník Okresního vlastivědného muzea v Blansku, **6–7**: 111–128.

Hanžl, P. & Melichar, R. (1997): The Brno Massif: A section through the active continental margin or a composed terrane? – Krystalinikum, **23**: 33–58.

Havlík, J. & Mikeš, D. (2016): Srbský sifon – pojítko Rudického propadání a Býčí skály (Moravský kras). – Sborník Speleoforum, **35**: 9–15 & 127–131.

Hercman, H., Lauritzen S.E., Glazek, J. & Vít J. (1997): Proceedings of the 12th International Congress of Speleology. – pp. 45–47, Basel, Switzerland (Speleo Projects).

Hladil, J. (1983): The biofacies section of Devonian Limestones in the central part of the Moravian Karst. – Sborník geologických věd, řada G, **38**: 71–94.

Hladil, J. (1986): Trends in the development and cyclic patterns of Middle and Upper Devonian buildups. – Facies, **15**: 1–34.

Hrádek, M. & Ivan, A. (1974): Neotektonické vrásno-zlomové morfostruktury v širším okolí Brna. – Sborník Československé společnosti zeměpisné, **79**/4: 249–263.

Hypr, D. (1976): Nové objevy v Rudickém propadání – Velikonoční jeskyně. – Československý kras, **27**: 100–104.

Hypr, D. (1977): Fluviální sedimenty v jeskyni Barové. – Československý kras, **28**: 59–73.

Ivan, A. (1996): Morphotectonics of SE margin of the Bohemian Cretaceous Basin, two half-grabens and their surroundings north of Brno (Moravia). – Moravian Geographical Reports, **4**/1: 2–28.

Kadlec, J., Hercman, H., Nowicki, T., Glazek J., Vít J., Šroubek P., Diehl J.F. & Granger, D. (1999): Dating of the Holstejnska Cave sediments (Moravian Karst). – In: Vit, J. (ed.): Abstracts of the 4th International Meeting of Cavers in the Moravian Karst and the 2nd National Speleological Congress, Jedovnice 1999. – pp. 15–18, Praha (Czech Speleological Society).

Kadlec, J., Herzman, H., Beneš, V., Šroubek, P., Diehl, J.F. & Granger D. (2001): Cenozoic history of the Moravian Karst (northern segment): cave sediments and karst morphology. – Acta Musei Moraviae, Sci. naturales, **86**: 11–160.

Kettner, R. (1960): Morfologický vývoj Moravského krasu a jeho okolí. – Československý kras, **12**: 47–84.

Květ, R. (1974): Kluftzonen und planetare Aquidistanz-Störungssysteme. – Zeitschrift für geologische Wissenschaften, **5**: 561–597.

Lauritzen, S.E. & Lundberg, J. (2000): Solutional and erosional morphology. – In: Klimchouk, A.B., Ford, D.C., Palmer, A.N. & Dreybrodt, W. (eds): Speleogenesis. Evolution of karst aquifers. – pp. 408–426, Huntsville (National Speleological Society).

Lauritzen, S.E. (2013): Paragenesis: the "royal mark" of subglacial speleogenesis. – In: Fillipi, M. & Bosák, P. (eds): 16th International Congress of Speleology: Czech Republic, Brno July 21–28, 2013: Proceedings. – pp. 366–367, Prague (Czech Speleological Society).

Lysenko, V. & Slačík, J. (1975): Chemismus genetisch verschiedener Sinterformen in den Koneprusy-Höhlen (CSSR). – Annales de Spéléologie, **30**/4: 711–717.

Mikeš, D., Havlík, J. & Gregor, V.A. (2015): Průstup jeskyněmi Jedovnického potoka ze vchodu do Býčí skály do východu z Rudického propadání a zpět dne 4. července 2015. – Sborník Muzea Blansko, **2015**/1: 5–15, 39–48.

Musil, R. (1993): Moravský kras labyrinty poznání. – 336 pp., Adamov (Jaromír Bližňák GEO program).

Musil, R. (1997): Ende des Pliozaens und unteres bis mittleres Pleistozaens des Bruenner Beckens. – Acta Musei Moraviae, Scientiae geologicae, **96**/1–2: 93–107.

Musil, R. (2009): Deposition and erosion stages in the Moravian Karst. – Acta Musei Moraviae, **94**: 151–165.

Musil, R., Děkanovský, O., Ivanov, M., Doláková, N., Mrázek, J., Juřičková, L. & Lundberg, J. (2018): Dagmar Cave (Czech Republic, Moravian Karst), a unique palaeontological site of the Cromerian Interglacial. – Quaternary International, in press.

Panoš, V. (1961): Kvartérní krasové procesy v severní části Moravského krasu. – In: Jelínek, J., Dočkalová, H., Hank, V., Hrubý, V., Kux, Z., Musil, R., Sejbal, J. & Stehlík, J. (eds): Symposion o problémech pleistocénu. (Anthropos, 14, N. S. 6). – pp. 77–92, Brno – Moravian Museum Brno).

Pasini, G. (2009): A terminological matter: paragenesis, antigravitative erosion or antigravitational erosion? – International Journal of Speleology, **38**/2: 129–138.

Pavlides, S.B. (1989): Looking for a definition of neotectonics. – Terra Nova, **1**/3: 233–235.

Pelíšek, J. (1980): Kalcitové výplně puklin ve vápencích Moravského krasu. – Československý kras, **31**: 113–115.

Renault, P. (1968): Contribution a l'étude des actions mechaniques et sedimentologiques dans la spéléogenèse. – Annales de spéléologie, **22**: 5–21, 209–267; **23**: 259–307, 529–596; **24**: 313–337.

Renault, P. (1970): La formation des cavernes. – "Que sais-je?", No° 1400. – 126 pp., Paris (Presses universitaires de France).

Skácelová, Z. & Havíř, J. (1998): Earthquakes on the eastern margin of the Bohemian Massif recorded by the stations of the IPE Brno. – Exploration Geophysics, Remote Sensing and Environment, **2**: 16–21.

Slačík, J. (1975): Lumineszenz-Typologie des Kalzites und anderer Hohlenminerale. – Annales de Spéléologie, **30**/4: 753–759.

Slačík, J. **(**1982): Příspěvek k chemismu primárních kalcitů v moravských jeskyních (A contribution to the chemism of primary calcites in Moravian caves). – Československý kras, **33**: 27–33.

Slobodník, M. (2000): Hydrotermální mineralizace (Hydrothermal mineralization). – In: Motyčka, Z., Polák, P., Sirotek, J. & Vít, J. (eds): Amaterská jeskyně. (The Amaterska Cave). – pp. 117–121, 181, Brno (Česká speleologická společnost).

Špaček, P., Sýkorová, Z., Pazdírková, J., Švancara, J. & Havíř, J. (2006): Present-day seismicity of the south/eastern Elbe fault system (NE Bohemian Massif). – Studia Geophysica et Geodaetica, **50**: 233–258.

Špaček, P., Valenta, J., Táborík, P., Ambrož, V., Urban, M. & Štěpančíková, P. (2017): Fault slip versus slope deformations: Experience from paleoseismic trenches in the region with low slip-rate faults and strong Pleistocene periglacial mass wasting (Bohemian Massif). – Quaternary International (in press).

Vita-Finzi, C. (1986): Recent earth movements: An introduction to neotectonics. – 226 pp., London (Academic Press Inc.).

Zukalová, V. & Chlupáč, I. (1982): Stratigrafická klasifikace nemetamorfovaného devonu moravskoslezské oblasti. – Časopis pro mineralogii a geologii, **27**/3: 225–241.